<u>A STATISTICAL COMPARISON OF SIDEWALK SLOPES DERIVED FROM MULTI-RESOLUTION DIGITAL ELEVATION MODELS IN SUPPORT OF ACCESSIBILITY</u>

by

Robin E. Rodgers
A Thesis
Submitted to the
Graduate Faculty
of
George Mason University
in Partial Fulfillment of
The Requirements for the Degree
of
Master of Science
Geoinformatics and Geospatial Intelligence

Committee:

___________________________	Dr. Kevin M. Curtin, Thesis Director
___________________________	Dr. Matthew T. Rice, Committee Member
___________________________	Dr. Arie Croitoru, Committee Member
___________________________	Dr. Anthony Stefanidis, Department Chair
___________________________	Dr. Donna M. Fox, Associate Dean for Student Affairs, College of Science
___________________________	Dr. Peggy Agouris, Dean, College of Science
Date: ______________________	Fall Semester 2015 George Mason University Fairfax, VA

A Statistical Comparison of Sidewalk Slopes Derived from Multi-Resolution Digital Elevation Models in Support of Accessibility

A Thesis submitted in partial fulfillment of the requirements for the degree of Master of Science at George Mason University

by

Robin E. Rodgers
Bachelor of Science
The University of Georgia, 2007

Director: Kevin M. Curtin, Associate Professor
Department of Geography and GeoInformation Science

Fall Semester 2015
George Mason University
Fairfax, VA

DEDICATION

This work is dedicated to my father, Frank, and to my beloved feline, Tux. Both are now gone, but certainly not forgotten.

ACKNOWLEDGEMENTS

I would like to thank my committee, Dr. Kevin Curtin, Dr. Matthew Rice, and Dr. Arie Croitoru, for the time they took to assist me throughout the research process. I would also like to thank my family, friends, and colleagues who provided continuous support and encouragement: Mr. Jose Lopez, Mrs. Elaine Rodgers, Dr. Jim Shine, Ms. Katy Kash, Mr. Scot Cleveland, and Mr. Roger Brown.

TABLE OF CONTENTS

LIST OF TABLES

LIST OF FIGURES

LIST OF EQUATIONS

LIST OF ABBREVIATIONS AND SYMBOLS

3D Elevation Program..3DEP
Americans with Disabilities Act ....ADA
Americans with Disabilities Act Accessibility Guidelines.................................... ADAAG
Department of Transportation.. DOT
Digital Elevation Model..DEM
Digital Terrain Model ....DTM
Environmental Systems Research Institute...ESRI
Federal Highway Administration..FHWA
Geographic Information Systems .... GIS
Geography and GeoInformation Science...GGS
George Mason University .... GMU
Global Coordinate System ....GCS
Ground Control Point...GCP
Interferometric Synthetic Aperture Radar ....IfSAR
Light Detection And Ranging...LiDAR
Meter(s).. m
National Elevation Dataset .... NED
National Map Viewer.. NMV
National Oceanic and Atmospheric Administration ....NOAA
North American Datum...NAD
North American Vertical Datum...NAVD
Percent.. %
Portable Document Format .... PDF
Root Mean Square Error ....RMSE
Three-Dimensional 3D
United States .... U.S.
United States Access Board ....USAB
United States Geological Survey .... USGS
Universal Transverse Mercator...UTM
Virginia ....VA

ABSTRACT

A STATISTICAL COMPARISON OF SIDEWALK SLOPES DERIVED FROM MULTI-RESOLUTION DIGITAL ELEVATION MODELS IN SUPPORT OF ACCESSIBILITY

Robin E. Rodgers, M.S.

George Mason University, 2015

Thesis Director: Dr. Kevin M. Curtin

Sidewalk slope is a major factor taken into consideration when visually or mobility impaired pedestrians select a route to their destination. In an effort to improve campus accessibility, a testbed pedestrian routing environment, called the George Mason University (GMU) Geocrowdsourcing Testbed, has been developed by researchers in the Department of Geography and GeoInformation Science (GGS) at GMU in Fairfax, Virginia. In order to determine how to best incorporate slope as an attribute in the testbed's sidewalk network, this research considers the effect that using Digital Elevation Models (DEMs) of varying spatial resolutions has on the accuracy of slope calculations. Lower resolution DEMs are often free and more easily acquired than higher resolution DEMs, such as those derived from Light Detection And Ranging (LiDAR). Therefore, if a lower resolution DEM sufficiently captures variations in slope, it may be deemed acceptable to use for this type of application, when a high resolution DEM is not

available. To test this proposition, slope values for the sidewalk network were derived from four DEMs with the following resolutions: 1/3 arc-second (about ten meters); five meters; 1/9 arc-second (about three meters); and one meter (m). The slope values from the lower resolution DEMs were statistically analyzed and compared to the high resolution 1 m DEM and to each other to detect significant differences. The results conveyed that the differences between the slope values derived from the lower resolution DEMs and the slope values calculated from the 1 m DEM were statistically significant. Consequently, it was concluded that, for the incorporation of slope in the GMU Geocrowdsourcing Testbed, a high resolution (1 m or higher) DEM needs to be used for slope calculations, to provide the most accurate results for visually and mobility impaired pedestrian routing.

CHAPTER ONE

1.1 Introduction

A research team with the Department of Geography and GeoInformation Science (GGS) at George Mason University (GMU) in Fairfax, Virginia (VA) has developed an application called the GMU Geocrowdsourcing Testbed (Figure 1). It is designed to collect transient navigation obstacle information and provide routing and data visualization, specifically for visually and mobility-impaired students (Rice, Curtin, Paez, Seitz, & Qin, 2013). Crowdsourcing is incorporated to allow contributors to provide up-to-date information about barriers (such as construction cones) that are present, whether temporarily or long-term, along pedestrian routes across campus. It is likely that visually and mobility impaired students traverse paths with which they are familiar. Thus, the presence of unexpected obstructions can be quite inconvenient, not to mention potentially dangerous, and the student will have to find an alternate, accessible route. The GGS Department's testbed web application can dynamically provide alternate routes based on obstacle information entered. However, these new routes may present other challenges, such as directing students to travel on sidewalks that have steeper slopes and may not be easy to manage. For safety, students requiring accessible paths may opt to take a longer route rather than a shorter one, if that means not having to deal with more precarious sidewalk conditions.

Earlier versions of the testbed did not incorporate slope, and it was discovered, upon asking students to validate the results provided by the routing algorithm, that slope was an important factor that had been neglected. By incorporating the slope of sidewalks and including it as an impedance factor in the testbed routing algorithm, route options, with or without obstacles present, have a higher chance of being optimal for the student, with respect to the quickest, safest path. While the current routing algorithm used in the testbed does take slope into account as an impedance factor, it is possible that the slope values are not as accurate as they should be to provide a truly accessible route. The slope values currently in use were derived from a 1/9 arc-second (about three-meter resolution) digital elevation model (DEM) obtained from the United States Geological Survey's (USGS's) National Elevation Dataset (NED).

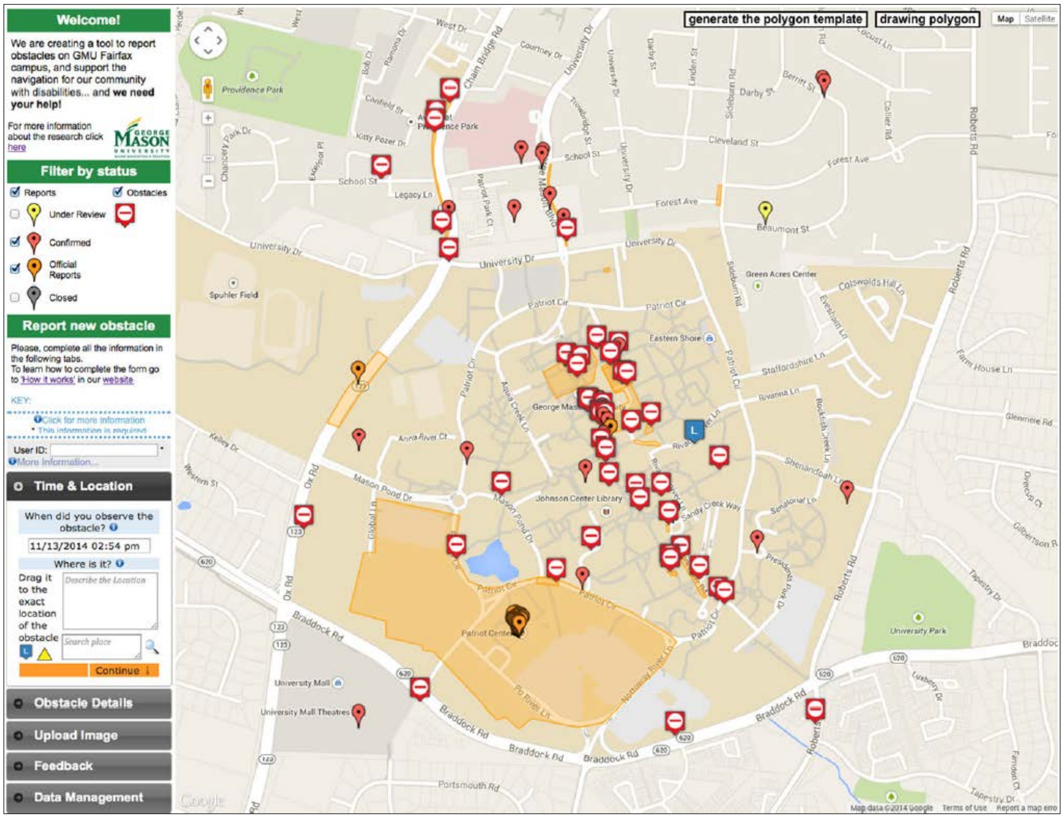

Figure 1 GMU Geocrowdsourcing Testbed (Source: Qin et al., 2015)

GMU has produced a Physical Accessibility Map of the Fairfax Campus (Figure 2), and while it does provide students with a good idea of the accessible (Americans with Disabilities Act [ADA] compliant) sidewalks, entrances, and parking spots across campus, it is static in nature (a Portable Document Format [PDF] file). As such, it cannot incorporate dynamic obstacle information that may impact the route a disabled student would take. It is also not frequently updated. As of November 2015, the map available online was revised in August 2012. The ADA compliant sidewalks data and other map data could not be acquired for analysis and comparison with the slope results derived in this research because the data were not available in a file format supported by Geographic

Information Systems (GIS) software. Fortunately, the GMU Geo-crowdsourcing Testbed will allow the same information to be available to students in an interactive environment, enhancing their awareness of current campus conditions and giving them the security of knowing that an alternate route to their destination can be calculated dynamically based on the latest information available.

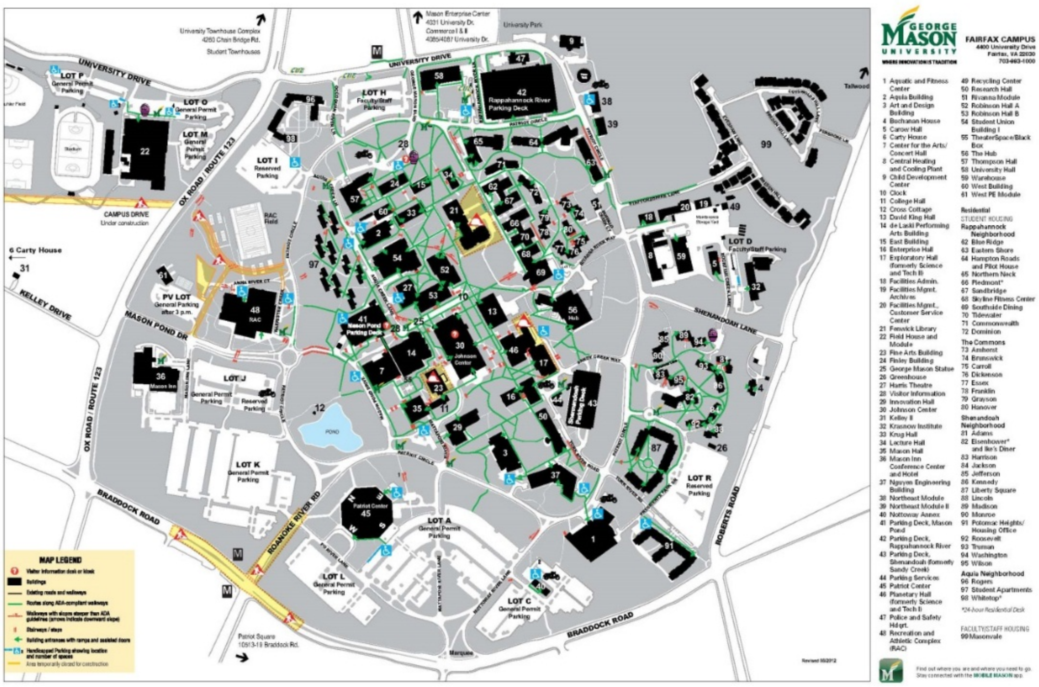

Figure 2 GMU Fairfax Campus Physical Accessibility Map (Source: GMU, 2012)

Elevation data are required in order to calculate slope using GIS software. Light Detection And Ranging (LiDAR) can provide high resolution elevation data, but it is typically not freely available, and, even if it is, it may not be available for the desired study area. Other elevation data, such as the USGS NED, are more readily available, but the quality of the resolution is lower. Standard lower resolution DEMs available through the USGS include 2 arc-second (about 60 meters), 1 arc-second (about 30 meters), 1/3 arc-second (about 10 meters) and 1/9 arc-second (about 3 meters) DEMs. In January 2015, a new project called the 3D Elevation Program (3DEP), managed by the USGS, began. Its goal is to have free, publicly available high resolution elevation data (LiDAR) coverage of the entire United States (U.S.) by 2022 (Carswell, 2013). In October 2015, high resolution 1 meter (m) DEMs became available over GMU and the surrounding areas. Nevertheless, much of the country still does not have freely available high resolution elevation data.

The objective of this research was to determine if the slope results from any of the lower resolution DEMs considered were comparable to the results obtained from the high resolution 1 m DEM. This was achieved by visually and statistically comparing slope values calculated from three lower resolution (3 m, 5 m, and 10 m) DEMs to the slope values from the LiDAR-derived 1 m DEM, which was used as the ground truth dataset. If the slope results from one of the lower resolution DEMs were acceptable for this application (namely, determining the slopes of sidewalks in order to identify them as ADA compliant), then using a lower resolution DEM would be a viable option, at least until a higher resolution DEM becomes freely available over the desired area. The study area selected for this endeavor was the GMU main campus in Fairfax, VA.

1.2 Content Organization

This research is divided into several chapters in order to present the information in an organized manner. Chapter 2 discusses relevant background information, as well as similar research that has been conducted in related applications. Chapter 3 describes the datasets that were acquired to perform the analysis and identifies the selected study area. Chapter 4 steps through the data preparation process and analytical methods used to assess the relative accuracies of the slope values. Since ground truth data for sidewalk slopes were not available, DEM elevation values were assessed for accuracy by comparing them to field surveyed spot elevation points using the root mean square error (RMSE). Given the high accuracy of the 1 m DEM, the slope values derived from it were considered to be ground truth, enabling accuracy assessments of slope values derived from the other DEMs using GIS software to be conducted. The differences in the slopes produced from each DEM were first observed visually by color-coding the sidewalks by percent slope categories. Statistical comparisons were then made using paired *t*-tests and Wilcoxon signed-rank tests to identify significant differences in slope results between DEM pairs. Chapter 5 outlines the results obtained from the analysis and then moves into a discussion. All of the lower resolution DEMs provided slope results that were statistically significant when compared with the slope results obtained from the high resolution DEM. Therefore, for similar applications at this scale requiring a high level of slope detail to be captured, a high (1 m or higher) resolution DEM provides the most accurate results. Lastly, Chapter 6 presents conclusions and recommended future research. Ultimately, it is the combination of a clean, systematically digitized sidewalk dataset, a well-chosen slope calculation algorithm, and accurate, high resolution elevation data that leads to trustworthy slope results. In other words, it is the quality of the input data that will determine the quality of the final results.

CHAPTER TWO

2.1 Definitions: Slope and Cross-Slope

Ideally, when conducting pedestrian routing, two types of slope need to be taken into account: slope (also called grade) and cross-slope. Slope is defined as the slope parallel to the direction of travel. It is calculated by dividing the vertical change in elevation (rise) by the horizontal distance covered (run). Axelson et al. define (1999) running slope as the average slope along a contiguous slope, and maximum slope is defined as a limited section of path that exceeds the typical running slope. It is important to note that, if the maximum slope is relatively steep, even paths with moderate running slopes can be difficult to traverse. Figure 3 demonstrates this concept: the running slope (grade) is only 5 percent (%), but the maximum slope (grade) is 14%.

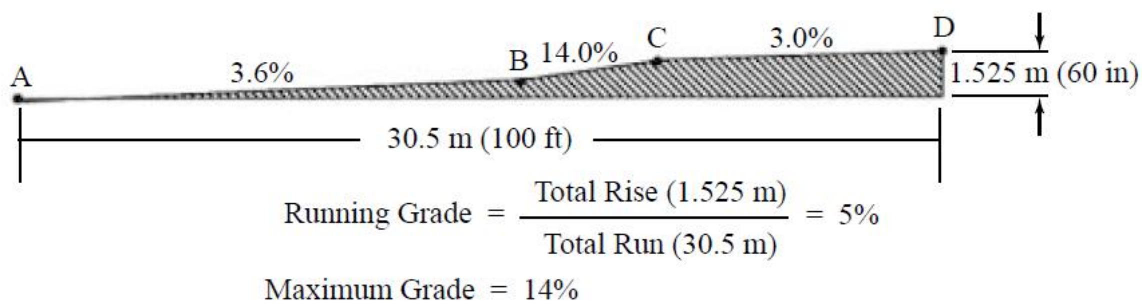

Figure 3 Running Grade versus Maximum Grade (Source: U.S. Department of Transportation [DOT] Federal Highway Administration [FHWA], 2014)

Cross-slope is the slope perpendicular to the direction of travel. Unlike grade, cross-slope can be measured only at specific points. Cross-slope is calculated by taking measurements at intervals throughout a section of sidewalk and then averaging the values. As prior research (Souleyrette, Hallmark, Pattnaik, O'Brien, & Veneziano, 2003), which will be discussed in the following paragraphs, has shown, even a high (approximately one foot) resolution DEM was unsuitable for accurately calculating cross-slopes on highway segments.

2.2 Challenges Faced by Pedestrians with Disabilities

Easily accessible sidewalks for pedestrians have become a necessity in increasingly urban environments, where mass transportation systems are often more convenient than commuting by privately owned vehicles. As challenging as it can be to identify an ideal pedestrian route, it is even more difficult for pedestrians with disabilities, whether physical or visual. When new routes have to be identified due to temporary obstacles (such as construction zones) that require pedestrians to take detours, both the slope and cross-slope of sidewalks encountered along the new route have a significant influence on whether or not a disabled pedestrian can traverse that route. Additional considerations must be taken into account when routing pedestrians with disabilities. The physical fitness level of the individual is a factor that influences the slope that the person feels comfortable scaling. Also, based on the direction of travel, the pedestrian may prefer taking one route to his or her destination and an alternative route back, depending on whether or not he/she is more comfortable descending versus ascending a given slope (Rice et al., 2014). In general, firm paths with smooth surfaces, free of steps, obstructions, and slopes are desirable. Given that it is usually not possible to meet all these criteria, standards have been put in place to help maintain safety for pedestrians with disabilities.

According to the U.S. Department of Transportation (DOT) Federal Highway Administration (FHWA), maximum slope should be measured over 0.61 m (two feet) intervals, since this is the approximate length of a wheelchair wheelbase or a single walking pace. For the average pedestrian, slopes of more than 6% require significant energy to travel up and considerable effort braking to go down (Price, 2012). For accessible paths, running slopes greater than 5% require hand rails, as specified in the Americans with Disabilities Act Accessibility Guidelines (ADAAG). A ramp is within the ADA requirements as long as the ramp maintains a running slope of 5% to a maximum of 8.33%. Slopes greater than 8.33% are difficult for disabled pedestrians (namely those using a wheelchair) to navigate for long distances. Therefore, maintaining a ramp slope as close to 5% as possible is recommended (United States Access Board [USAB]). Additionally, steep cross-slopes can make it difficult for wheelchair or crutch users to maintain lateral balance and can cause wheelchairs to veer downhill, roll into the street, or even tip over. Most sidewalks are built with some degree of cross-slope to allow water to drain into the street and to prevent water from collecting on the path. As such, the ADAAG state that cross-slopes should not exceed 2%.

An example of an easily overlooked consideration is the rate of change of grade: the change in grade over a given distance. In the sidewalk environment, rate of change of grade should not exceed 13%. An example of a 13% change in rate of grade occurs at a curb ramp if the slope of the gutter is 5% and the slope of the curb ramp is 8% (Figure 4). If the rate of change of grade exceeds 13% over a two-foot interval, the wheelchair footrests might not clear the ground. The stability of the pedestrian can also be significantly compromised, depending on the speed at which the wheelchair goes through the curb ramp (Axelson et al., 1999).

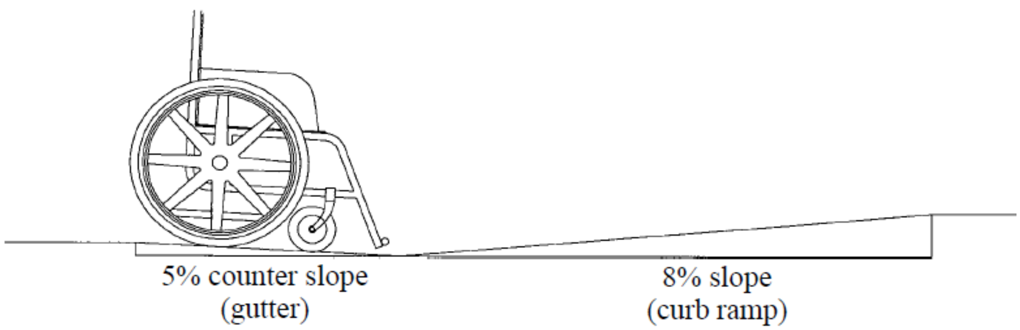

Figure 4 Rate of Change of Grade (Source: U.S. DOT FHWA, 2014)

With this information in mind, it is readily apparent that, when conducting routing specifically geared toward accommodating disabled pedestrians, slope is a major component. It must be incorporated as an impedance factor when routing algorithms are implemented in order to successfully offer alternate routing solutions. The ideal situation would be to calculate slope every 0.6 m, as per ADA guidelines, but this is often not an option, due to financial constraints and the availability of personnel. A more feasible solution is to use available elevation data to calculate slopes as accurately as possible.

2.3 A Brief Review of DEMs, Contours, and LiDAR

Since slope is derived from elevation data, it would be beneficial to briefly review the differences between some common elevation dataset types. DEMs, or Digital Elevation Models, are three-dimensional (3D) representations of continuous elevation values over a topographic surface. The data collected to create DEMs are commonly obtained through remote sensing techniques, such as radar satellites, or from aerial photogrammetry. Contours, typically produced from direct field surveys, are lines that connect points of equal elevation based on a vertical datum, or reference (often mean sea level). Interpolation techniques can be used to produce a continuous surface similar to a DEM from contours, but it is more appropriate to call a contour-derived dataset a digital terrain model (DTM). For simplicity, however, this research will refer to contour-derived DTMs as DEMs. In GIS, the raster data model represents data that vary continuously, and it is made up of a regular grid of cells, also called pixels. Elevation rasters have a single value, representing elevation, assigned to each cell.

The quality of a DEM depends on how accurate the elevation value is for each cell. One primary factor that affects accuracy is the resolution of the DEM. The resolution describes the size of the cells in the raster. For example, a 10 m DEM contains cells that are ten meters by ten meters, and each cell contains an elevation value. Smaller cells tend to capture more terrain variation. Figure 5 shows an example of the increase in the level of detail captured as cell size decreases. For this reason, Light Detection And Ranging, or LiDAR, is one of the most accurate data collection methods used to produce DEMs, given that cell size is commonly one meter or less. LiDAR is a high resolution remote sensing technique in which laser pulses are emitted at the target, and the returns are analyzed to determine elevation. Aerial and terrestrial (a vehicle, for example) platforms can both be used for LiDAR collections. The output is a dense point cloud, and the spacing of the points (every half meter, every one meter, et cetera) should determine the minimum cell size of the DEM that is generated.

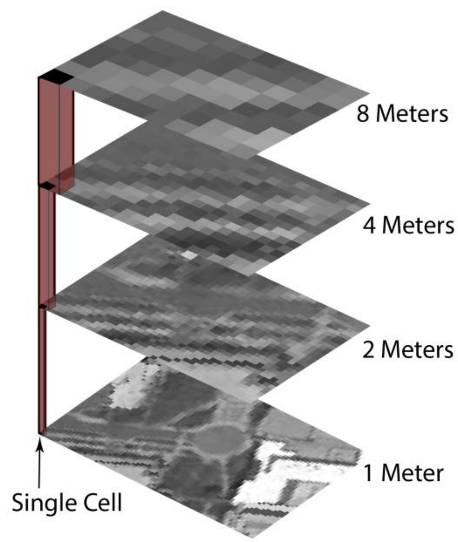

Figure 5 Raster Resolution: detail increases as cell size decreases

2.4 Slope as a Factor for ADA Sidewalk Compliance and Pedestrian Routing

The Public Works Department of the City of Clayton, Missouri, conducted a study in 2014 to determine their sidewalk compliance with ADAAG. Using a laser sensor system mounted on a Segway, they were able to measure the sidewalk surface at a rate of 10,000 records per second. The system captured highly detailed information about slope, cross-slope, and small surface variations. This extremely accurate data provided by the laser system allowed the city to identify which sidewalks were in compliance with ADAAG. The ADAAG does provide exceptions for non-compliance due to technical infeasibility. For example, if sidewalks follow the natural topography of the area, it may not be possible to meet grade compliance. The City of Clayton used a LiDAR DEM to derive slope values for the centerlines of streets adjacent to any non-compliant sidewalks. This way, they could show that some of the non-compliant sidewalks were simply following the roadway and area topography and could therefore be exempt from grade compliance due to technical infeasibility.

The difficulty that arises when trying to navigate across an area if a person requires a wheelchair has been recognized, and one solution has been to develop wheelchair navigation systems. In order to develop a personal wheelchair navigation system, sidewalk slope must be included as one of the attributes of the sidewalk network. It is preferable for the navigation system to allow the user to specify that he or she would like to avoid slopes, as wheelchairs are more sensitive to this attribute of the transportation network (Ding et al., 2007). Research conducted using a spatial database of the University of Pittsburgh campus area for a personal wheelchair navigation system used contour line data to calculate slope (Kasemsuppakorn & Karimi, 2009). The researchers recognized that slope was a required parameter for calculating impedance values when routing, as slope not only has an impact on accessibility, but also on safety for wheelchair users. In a similar study, researchers utilized GIS to develop bicycle and pedestrian networks on the University of Alabama campus to assess how they facilitate travel for students and professors (Lundberg & Weber, 2014). In addition to impacting the safety factor, increases in slope can require more energy and increase travel time by reducing travel speed; therefore, once pedestrian networks are created, slope should be included as an impedance factor when assigning travel time to a line segment.

2.5 Analysis of DEMs with Varying Resolutions

The importance of including slope in pedestrian routing has clearly been demonstrated, but many organizations will not have the opportunity to use a terrestrial sensor system to obtain highly accurate data. Indeed, many organizations may not even have access to a high resolution 1 m LiDAR DEM, either due to financial constraints or unavailability over the study area. While this should change in the near future with the USGS's 3DEP project, for the present, it is worthwhile to determine if lower resolution DEMs may be used for deriving slope values with accuracies suitable for disabled pedestrian routing.

Landslide susceptibility and hydrology are other applications for which slope is an important factor. A study considering landslide susceptibility commented on the use of high and lower resolution DEMs for slope calculations, concluding that higher resolution DEMs provide better determination of slope instabilities (Fuchs, Torizin, & Kühn, 2014). However, there is a catch; the higher resolution DEM is only recommended if the other parameters required for high resolution mapping are available. The higher resolution DEM has a small impact (as far as model quality improvement) on poorly parameterized models, and its use in such a context is inefficient.

A hydrology study, in which hydrological features were derived from DEMs, discovered that higher resolution DEMs produced much better results than lower resolution DEMs derived from contour maps (Vaze, Teng, & Spencer, 2010). A higher resolution LiDAR DEM was also resampled to lower resolutions and compared to other DEMs of the same resolution, where it was discovered that the resampled LiDAR DEM provided higher accuracy and higher quality hydrological features than did the other DEM with the same resolution. Another study, in which slope and aspect were derived from DEMs for study areas in South America, confirmed that when performing a regional scale analysis, an original source lower resolution DEM is not optimal. Rather, if a lower resolution DEM is needed based on the scale of the application, and a higher resolution DEM is available, it can be resampled to a lower resolution (Grohmann, 2015). However, Li & Wong (2010) suggest that it would be best to evaluate lower resolution DEMs derived from higher resolution data to confirm that they are, in fact, superior to other data sources with lower resolutions, versus making that assumption.

When making a determination about the appropriate DEM resolution to use for a particular application, one study explained that the grid cell size of the DEM must be the same as or less than one-half the size of the smallest geographic unit to be investigated. Therefore, to calculate slope over a five meter segment, the DEM utilized should have a resolution of 2.5 meters or less (Warren, Hohmann, Auerswald, & Mitasova, 2004). On the other hand, if the resolution is too high, slope variation may have a much higher level of detail than is relevant for the application being considered. It was also noted that in addition to resolution, the interpolation method and degree of smoothing applied during the creation of the DEM impacts the accuracy of slope calculations. As with any data analysis, the quality of the input data impacts the quality of the output results. For example, a 2008 study determined that the magnitude of slope errors resulting from elevation errors in a high resolution LiDAR DEM were only slightly smaller than errors in slope calculated from 10 meter and 30 meter resolution DEMs (Haneberg, 2008).

2.6 LiDAR Accuracy and Use as Ground Truth

A 2003 study conducted in Iowa utilized a LiDAR DEM (horizontal accuracy was 0.98 feet and vertical accuracy was 0.49 feet) to calculate running grade (slope) and cross-slope on tangent highway segments along Iowa Highway 1. These values were compared to field measurements for 10 test segments, each 100 feet in length, collected using an automatic level. It was observed that running grade on paved surfaces was within 0.5% of the surveyed value for most sections and within 0.87% for all sections (Souleyrette et al., 2003). Cross-slope estimates were less accurate, with LiDAR measurements deviating from field measurements by 0.72% to 1.65% on paved sections. The study concluded that running grade could be estimated to within 1% using LiDAR (clarifying that the specific application determines whether or not this is adequate), but that cross-slope cannot be estimated by LiDAR. While LiDAR may be the best option when it comes to estimating running grade, its acquisition for that sole purpose would not be practical, given that the process to collect and process LiDAR is fairly time-consuming and expensive. However, if LiDAR for the study area has already been collected for other purposes, as contracted by the state or another agency, it is certainly advantageous to use that dataset.

If a high resolution LiDAR DEM can provide fairly accurate results for slope, it may be possible, when comparing DEMs of varying resolutions, to use the LiDAR DEM in place of ground truth data, when ground truth data are not available, nor are there time and resources to collect ground truth. Airborne LiDAR can be collected over a wide range of spatial scales, while providing good spatial coverage at high resolution, with relatively little need for field time. A study published in 2006 documented the use of a LiDAR DEM with a resolution of two meters to extract ground control points (GCPs) and orthorectify old aerial photographs in order to produce DEMs from them. With a study area identified in northern England, GCPs were extracted from a LiDAR DEM and also collected using field survey methods. The results showed that while the use of LiDAR-derived ground control (also called ground truth) initially produced a DEM of inferior quality, increasing the number of GCPs used in the model produced results comparable to the field survey controlled DEM (James, Murray, Barrand, & Barr, 2006). A similar 2007 study for image orthorectification concluded that orthoimage accuracy achieved by using LiDAR data is superior to that achieved by using lower accuracy data sources, not to mention more cost effective (Liu, Zhang, Peterson, & Chandra, 2007). The RMSEs were 1.3 m for the LiDAR-orthorectified image and 7.26 m for the other data source, a 20 m resolution DEM.

In the National Oceanic and Atmospheric Administration (NOAA)-sponsored Rutland Ranch Ground Truth Survey for LiDAR Control conducted in 2006, ground truth checkpoints were compared with LiDAR points that were within three feet horizontally from the ground truth points. The result of the comparisons of the values indicated a vertical RMSE of 0.111 feet, which equated to vertical accuracy of 0.218 feet at the 95% confidence level (NOAA, 2006). This was within the vertical accuracy tolerance outlined in the Geometric Geodetic Accuracy Standards and Specifications published by the Federal Geodetic Control Committee in 1998.

Given the high accuracy results obtained in the previous studies, it is reasonable to opt to use high resolution LiDAR data as ground truth in the absence of available GCPs. Time and resources may not always be available for the collection of ground truth data. Ultimately, if a lower resolution DEM is able to provide reasonably accurate slope values for pedestrian routing, that will alleviate the required time and resources that are associated with high resolution data collection and processing.

CHAPTER THREE

3.1 Data Sources

Two data formats are used in this analysis: raster and vector. A raster represents data that vary continuously; it consists of cells, and each cell contains a value. Elevation and aerial imagery are examples of raster data, and common file extensions include TIF, JPEG, and IMG. A vector dataset represents data that have discrete boundaries—points, lines, and polygons—and their attributes. Only one of the three feature types is represented in a given dataset. For example, a polygon dataset could represent states, and the attributes might include name, area, and population. A popular and common standard geospatial vector data file format is the shapefile, developed by the Environmental Systems Research Institute (ESRI), and its extension is SHP. To use more familiar terms, vector data will be called feature data, and raster data will be referred to as elevation data, since the only raster datasets used in this analysis represent elevation.

3.2 Feature Data

A line shapefile containing the sidewalks throughout the GMU campus and the surrounding areas in Fairfax, VA was provided by the GGS Department (Figure 6). This shapefile, called the Pedestrian Network, represents the sidewalk centerlines and also contains attributes associated with the sidewalks, such as their length and accessibility (whether or not the sidewalk consisted of stairs or steep paths). It was generated by combining existing, incomplete campus sidewalk data with sidewalk data originally digitized by the Fairfax County GIS team from orthoimagery collected under the Virginia Base Mapping Program (Rice et al., 2015).

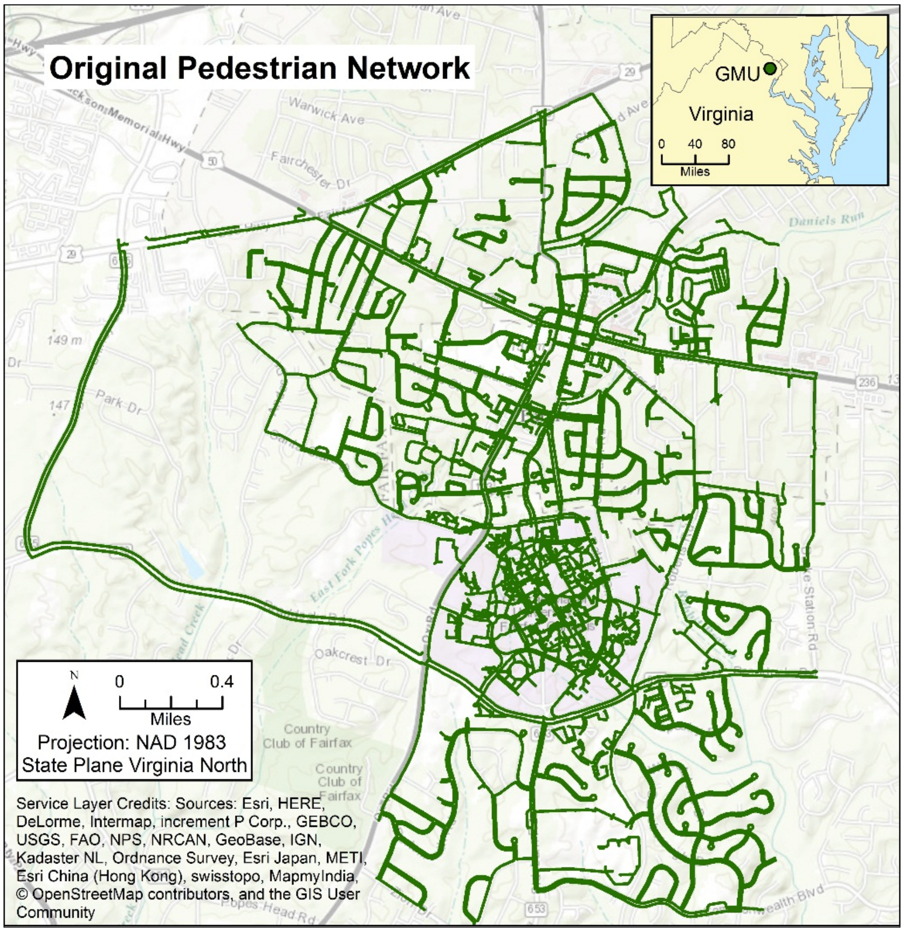

Figure 6 Original Pedestrian Network

Two additional files containing data collected for the GMU Facilities Division were provided: a point shapefile of spot elevations located throughout campus, and a line shapefile of elevation contour intervals (Figure 7). Campus spot elevations are collected by professional surveyors using surveying equipment, typically when new construction is completed on campus. The assumption is made that, to collect the spot elevations, they adhered to best practices and used field surveying equipment that provided high accuracy measurements. The contours were compiled by photogrammetric methods from aerial photography dated March 2010. The coordinate system is North American Datum (NAD) 1983 Virginia State Plane North, and the units are in feet. The vertical datum is based on the North American Vertical Datum (NAVD) of 1988. A GIS technician in the GMU Facilities Division updates the contours as needed using the spot elevations, and the contours were last updated in February 2015.

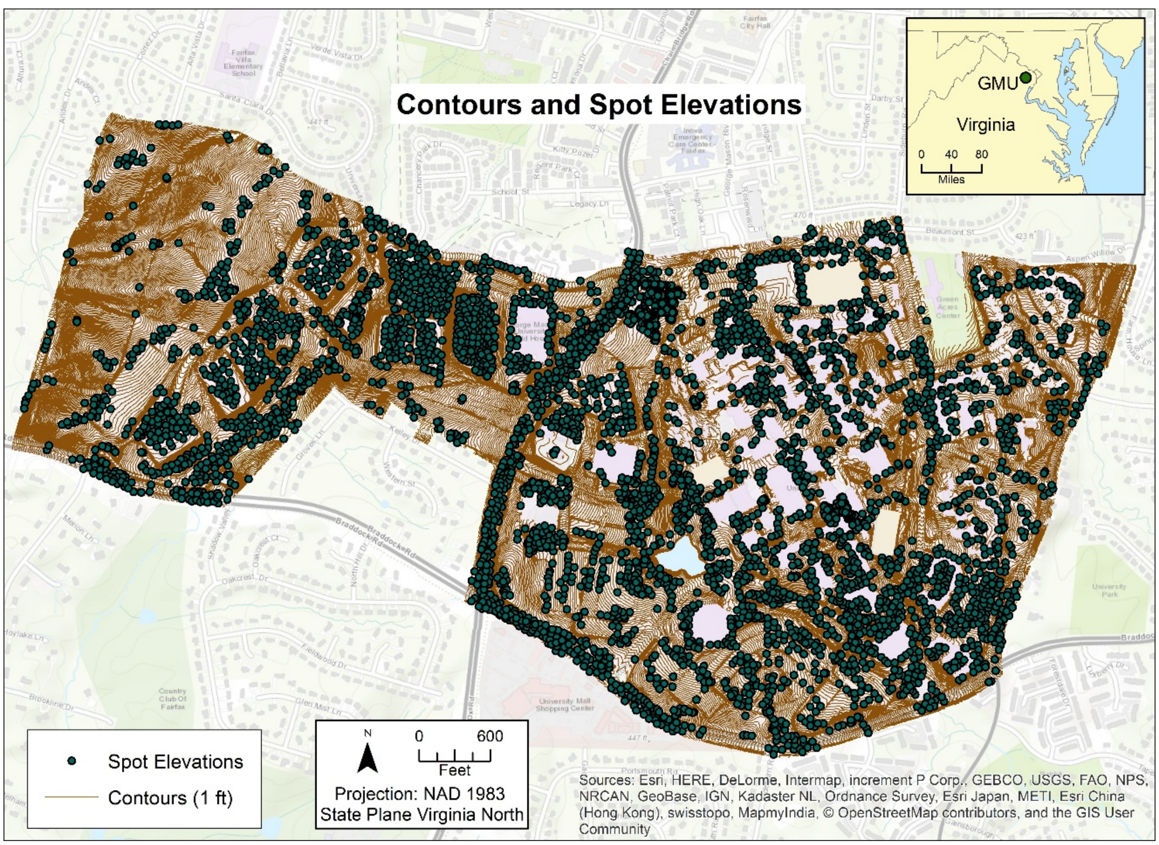

Figure 7 Contours and Spot Elevations

3.3 Elevation Data and Basemaps

Not long after this research began, USGS 3DEP LiDAR-generated, high resolution 1 m DEMs became available over GMU and the surrounding areas. These DEMs were downloaded using the USGS's National Map Viewer (NMV), which provides free geospatial data, including orthoimagery (aerial photographs), elevation, geographic names, hydrography, boundaries, transportation, structures, and land cover. The LiDAR points were collected in April 2014, and the DEMs were created in September 2015. The data quality level of the LiDAR points was Level 2. According to the 3DEP project specifications, Level 2 data have a nominal pulse spacing of 0.7 m and a vertical accuracy of 9.25 centimeters (Carswell, 2013). The nominal point spacing simply conveys that elevation points were collected every 0.7 m. The spatial reference of the 1 m DEMs generated from the LiDAR points is Universal Transverse Mercator (UTM), in conformance with the NAD of 1983, and the units are in meters. Each DEM tile is distributed in the UTM Zone in which it lies; in this case, all tiles acquired are in Zone 18 North. All elevation values are in meters and are referenced to the NAVD of 1988. To cover the GMU campus and the surrounding area, four 1 m DEM tiles were downloaded.

Lower resolution NED DEMs were also obtained from the USGS's National Map Viewer. Two DEMs with resolutions of 1/3 arc-second (about 10 m) and 1/9 arc-second (about 3 m) that covered the extent of the GMU campus and surrounding areas were downloaded. For simplicity, the 1/3 arc-second DEM will be referred to as the 10 m DEM, and the 1/9 arc-second DEM will be called the 3 m DEM. These DEMs are shown, along with the four 1 m DEM tiles, in Figure 8. NED DEMs are updated continually as new data become available. The 10 m DEM was last updated in 2014, while the 3 m DEM used in this research contains information collected in 2008 (the most recent 3 m DEM available over the area). The spatial references of both are geographic coordinates — the Global Coordinate System (GCS) — in units of decimal degrees, in conformance with the NAD of 1983. As with the 1 m DEM, elevation values are in meters and are referenced to the NAVD of 1988. Table 1 summarizes the information about the different DEMs. In the analysis conducted for this research, the 1 m USGS DEM was resampled to lower resolution 3 m, 5 m, and 10 m DEMs for comparison purposes. These resampled DEMs are denoted in Table 1 by an (R) beside them. All the DEMs used in this analysis were bare earth DEMs, which represent the topographic surface of the earth, as opposed to first return DEMs, which capture elevations of features on the earth's surface (such as trees and buildings) in addition to the topographic surface itself.

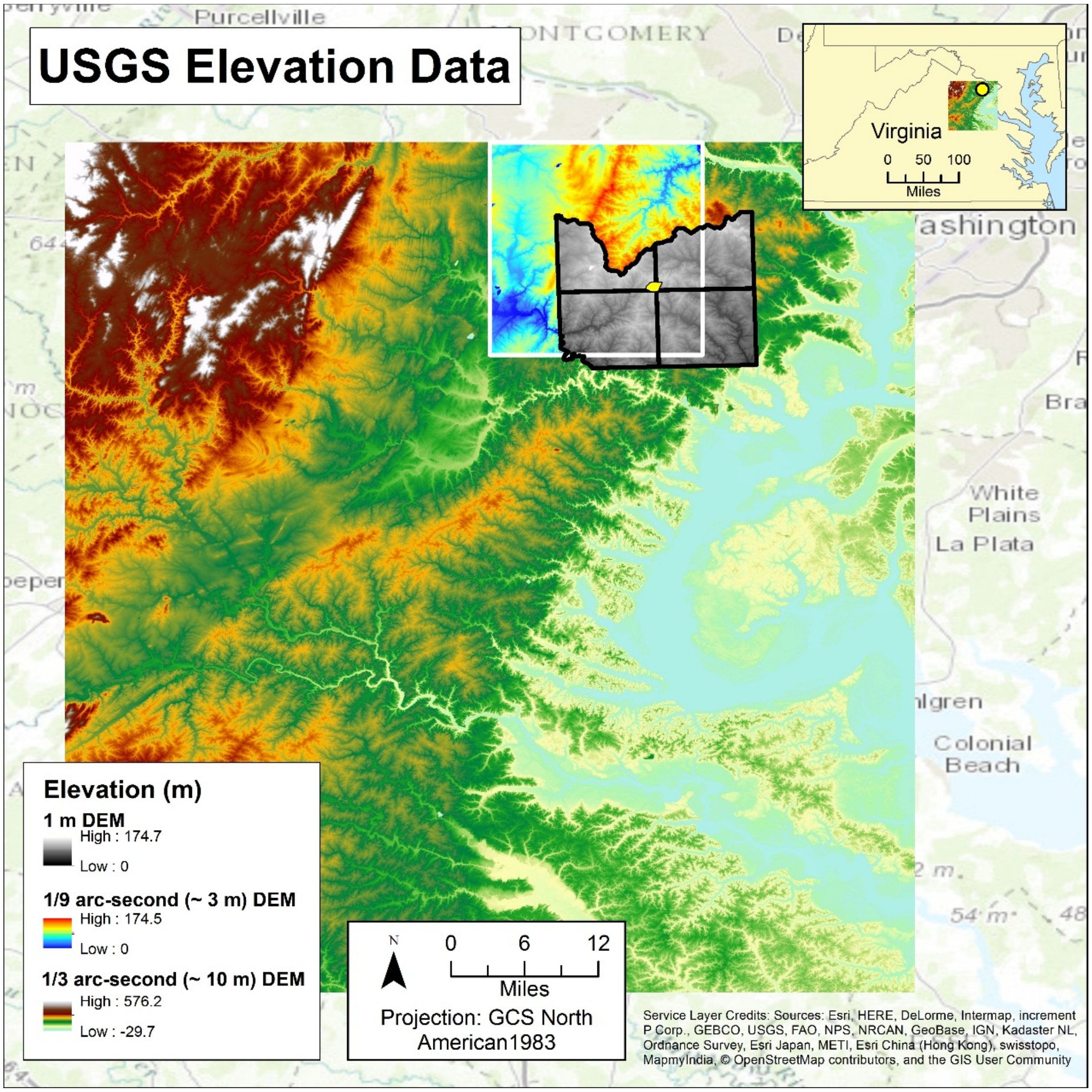

Figure 8 USGS DEMs. Yellow spot denotes GMU campus.

Table 1 Summary of Elevation Data (Sources: USGS 3DEP Product Metadata and GMU Facilities Division)

DEM	Retrieved from	Data Collection: Start Date	Data Collection: End Date / Last Updated	Data Source	Original Coordinate System	Coordinate System Measurement Unit
1 m, 3 m (R), 5 m (R), 10 m (R)	USGS NMV	April 2014	December 2014	LiDAR	NAD 1983 UTM Zone 18 North	meters
3 m	USGS NMV	March 2008	December 2008	LiDAR	NAD 1983 GCS	decimal degrees
5 m	GMU Facilities Division	not specified	February 2015	1 foot Contours created from March 2010 aerial photography	NAD 1983 VA State Plane North	feet
10 m	USGS NMV	1954	2014	diverse source data (typically derived from photogrammetrically produced contours or mass points and breaklines, or from Interferometric synthetic aperture radar [IfSAR])	NAD 1983 GCS	decimal degrees

To add context when viewing the Pedestrian Network and DEMs, two web map services made available by ESRI were identified to use as basemaps: World Imagery Map Service and World Topographic Map Service. The imagery service provides high resolution (0.3 m) imagery over the United States, and the topographic map service provides features such as boundaries, cities, water bodies, transportation, and buildings. These map services are free, publicly accessible, and frequently updated.

3.4 Study Area

The original Pedestrian Network provided by the GGS Department covered the entire GMU campus, as well as nearby areas in Fairfax, VA. The GMU campus is situated in the Piedmont Plateau physiographic region of Virginia, which is characterized by rolling hills (VA Department of Conservation and Recreation). Using the 1 m DEM as a reference, it was observed that elevations across campus range from 359 feet above mean sea level in the southeast corner to 472 feet in the western and northern parts of campus. In general, elevation increases going north and west. For the most part, undeveloped areas of campus are tree-covered, as seen in the aerial imagery shown in Figure 9. It was decided that the study area for the analysis would be limited to the Pedestrian Network sidewalks within the main campus of GMU. The study area, shown in Figure 10, is bounded by Ox Road to the west, Braddock Road to the south, Roberts Road to the east, and University Drive to the north.

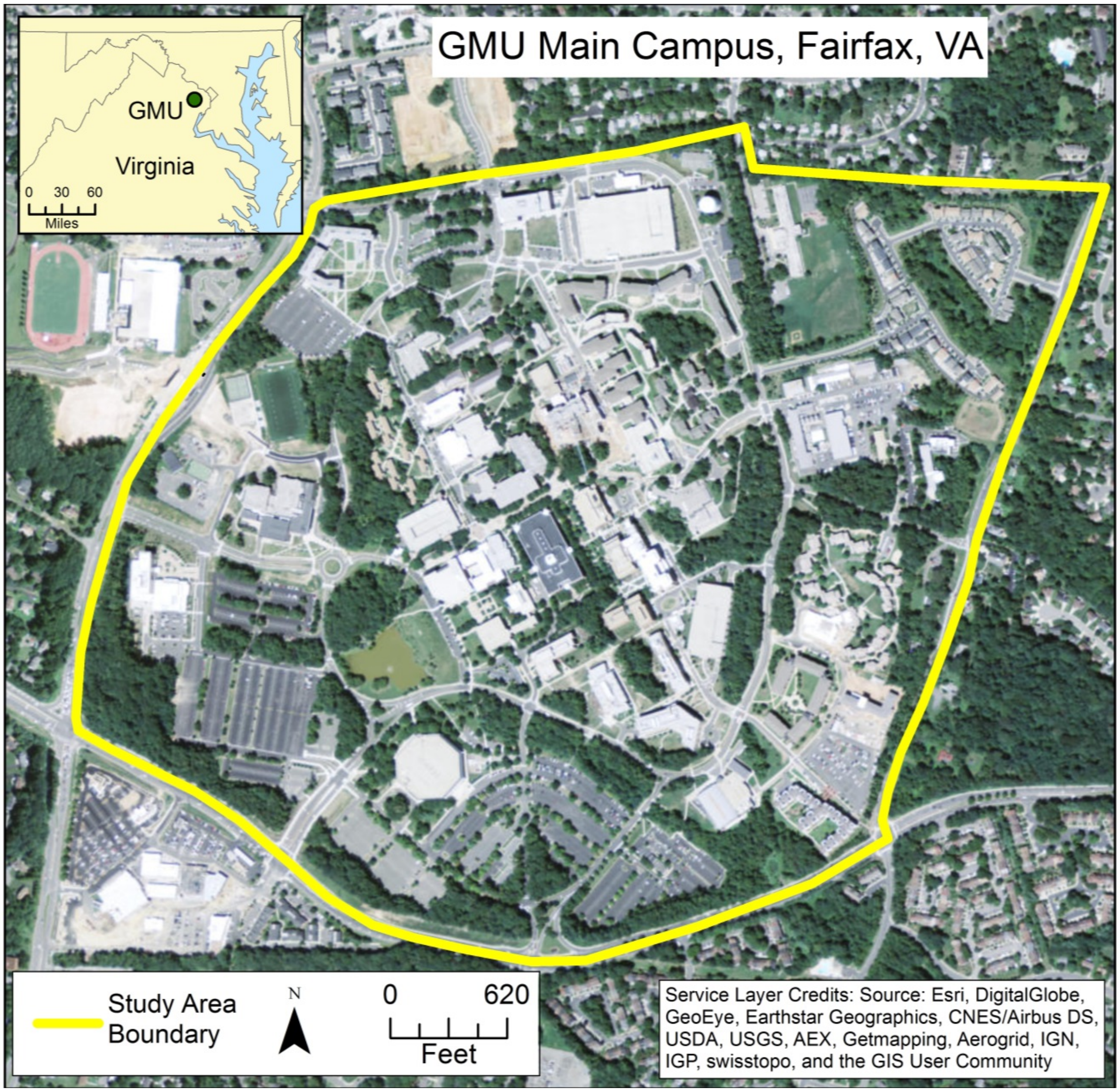

Figure 9 Aerial Imagery of GMU Campus within Study Area

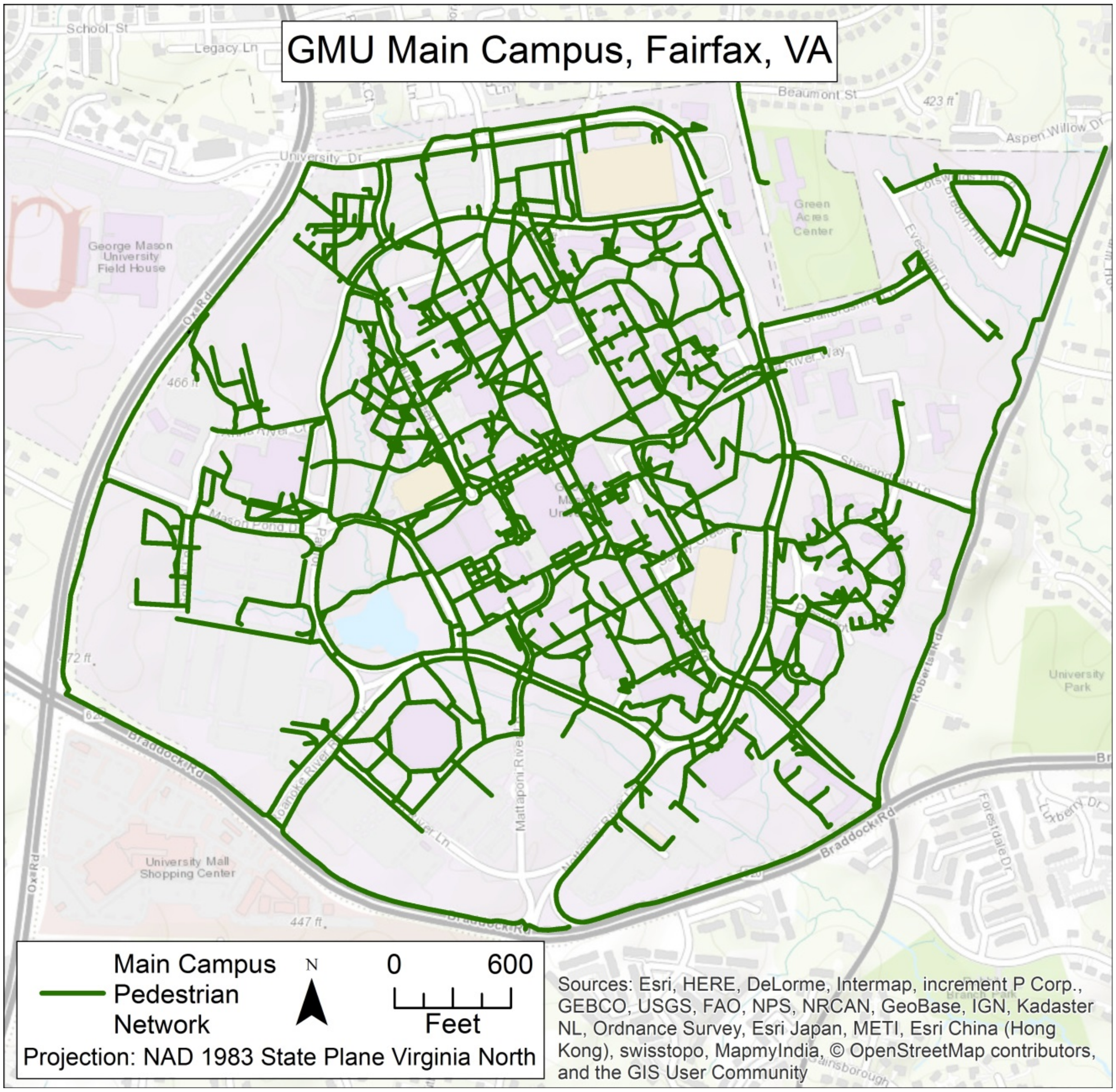

Figure 10 Study Area: GMU Main Campus Pedestrian Network

CHAPTER FOUR

4.1 Overview of Approach and Methods

One of the most important principles learned when performing an analysis is that the quality of the results is dependent upon the quality of the input data. Thus, the first priority was to assess the initial condition of the original datasets. The feature and elevation datasets were then processed as needed and clipped to the study area extent. Since the 1 m DEM was to be used in place of ground truth data, it was assessed for accuracy by comparing its elevation values with the same elevations captured by the field surveyed spot elevation points and calculating the RMSE.

Once the accuracy of the 1 m DEM was assessed, an appropriate slope calculation method was selected to obtain the slopes of sidewalks. Percent slope was determined by extracting elevation information (from each of the DEMs) corresponding to the line features of the Pedestrian Network. Differences in slope results between DEMs were tested for normality, as normality is an assumption of many statistical tests. The appropriate parametric test and its nonparametric counterpart were used to statistically compare the differences between slope results for each pair of DEMs to conclude whether or not the differences were significant. A general overview of the methods is presented in the flow chart shown in Figure 11, and the details are discussed in the following sections. In order to process and analyze the data, ESRI's ArcGIS Desktop

Advanced software (version 10.2.2) and its 3D Analyst and Spatial Analyst extensions were used.

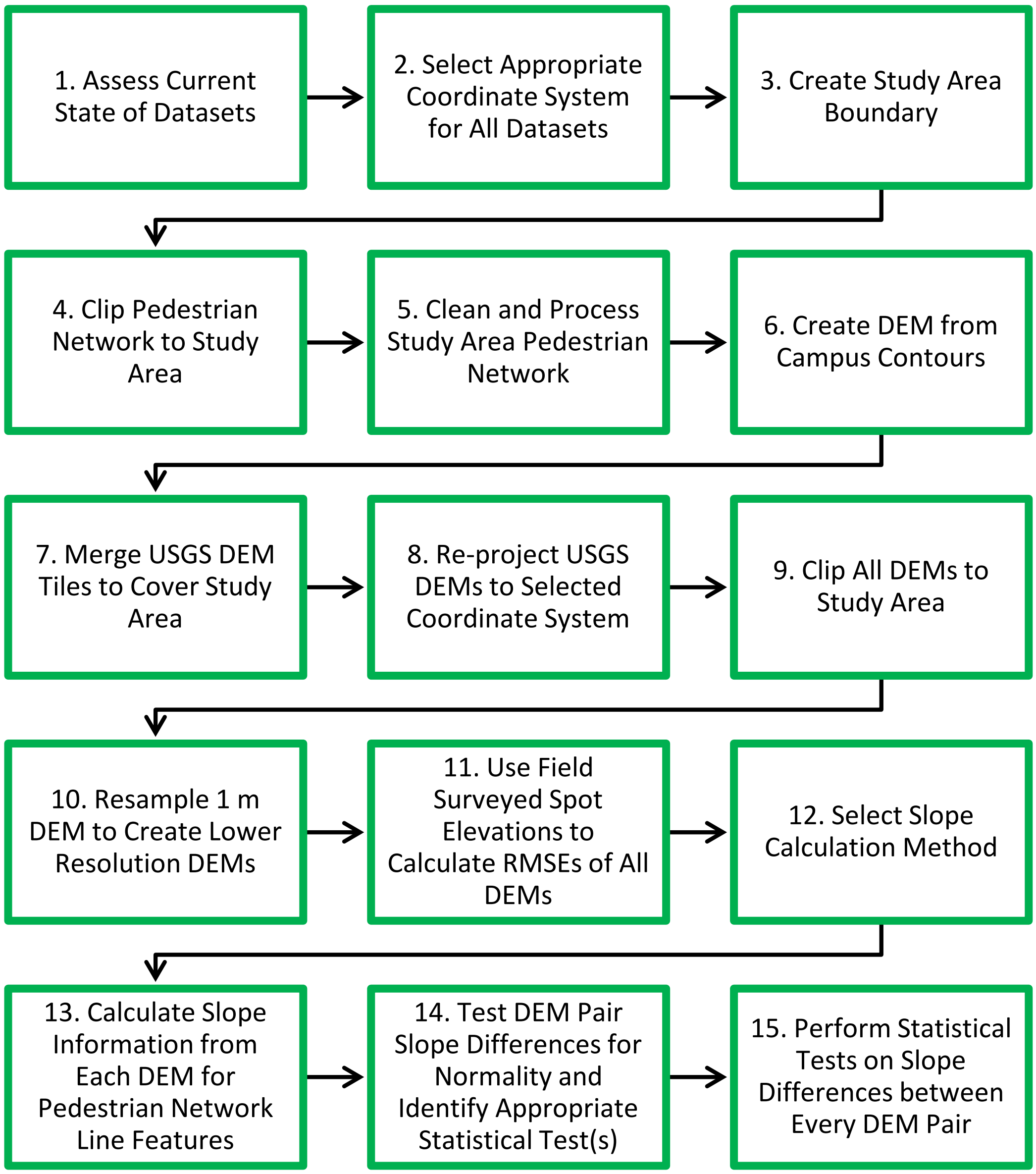

Figure 11 General Overview of Data Preparation and Analysis Methods

4.2 Assessment and Preparation of Feature Data

An understanding of the current state of the datasets was necessary before any data preparation and editing began. Additionally, the coordinate system that would be used throughout the analysis had to be identified, as it is best to convert all datasets to the same coordinate system before any analyses are performed. Since the ultimate goal of the results is to provide slope values for the testbed Pedestrian Network, the coordinate system of the Pedestrian Network (NAD 1983 Virginia State Plane North) was identified, so that all subsequent datasets could be converted to that coordinate system, if needed. To avoid processing more data than necessary, a boundary delineating the study area was created; only the feature data falling within this boundary were prepared for analysis.

The GMU Pedestrian Network was assessed to ensure the positional accuracy of the sidewalk lines, and the lengths of the line segments that made up the entire network were also evaluated. The network shapefile contained 3,489 line features. Visual observation of the network and its alignment with the same features on the image and topographic map services provided by ESRI, as well as a 2009 sidewalk centerline dataset acquired from Fairfax County Open Data, confirmed that the positional fidelity of the line features was acceptable. An inspection of the attribute table revealed that the length of the lines in the network varied greatly. Line lengths ranged from 0.16 feet to 2,327 feet, with an average length of 79 feet. The original network included the GMU campus sidewalks and sidewalks of the surrounding neighborhoods, as shown in Figure 6. The network was therefore clipped to the extent of the study area boundary to only include the sidewalks located within the main campus area (shown in Figure 10).

In an attempt to be more consistent when taking slope measurements, it was determined that a standard line length should be chosen. Ideally, slope would be calculated every two feet (0.6 m), as per guidelines set forth by the ADA, to capture small variations in the sidewalk that may be problematic for disabled pedestrians. However, that is not practical when the DEM resolutions (10 m, 5 m, 3 m, and even 1 m) are not high enough to accurately capture that level of detail. Shorter lines mean more line features, which will also lead to an increase in the complexity of calculations, especially during routing. Waze, Google's navigation mobile application, and Routino, an open source routing application using Open Street Map, both recommend that street segments be at least 5 m (16.4 feet) in length, for processing speed and routing accuracy. Since the lowest resolution DEM used in this analysis was 10 m, though, the sidewalk line features needed to be long enough to allow the 10 m DEM to capture variations. Keeping in mind the guideline mentioned by Warren et al. (2004) that the size (length in this case) of features should be at least twice that of the frequency of expected change in the underlying raster, the GMU Pedestrian Network was divided into line lengths of 20 m (65.6 feet). Since the lowest resolution DEM used was 10 m, then change could be expected every 10 m, so the line features would need to be at least 20 m long. To accomplish this, a point dataset with points spaced 20 m apart was created using a free function of an ArcGIS extension called ET GeoWizards, and these points were used to split the line features (sidewalks) in the Pedestrian Network. Due to the fact that not all lines were evenly divisible by 20, numerous shorter, remainder line features were produced. These short lines were inspected, and all those less than 5 m in length were merged with an adjacent line, in order to minimize the number of very short line features. One exception made was that short line features classified as “stairs” or “steep paths” were not merged with adjacent lines, if the adjacent lines were not also stairs or steep paths. Thus, there are a few line features (2.7%) that are under 5 m; some (18.5%) ended up being between 5 m and 10 m; a good number of lines (27.7%) are greater than 10 m and less than 19.8 m in length; and a slight majority of lines (51.1%) are 19.8 m or greater, with the maximum line length being 26.8 m (88 feet). The total number of line features in the study area Pedestrian Network was 2,887.

With the pedestrian network in the desired condition, attention could then be turned to the campus contour dataset. Since the coordinate system of the contours was the same as that of the network, no changes needed to be made. The contours were in one-foot (0.3 m) intervals, meaning that moving from one contour interval line to the next resulted in either an elevation increase or decrease of one foot. The first step taken was to create a DEM from the contours, so that this dataset could be in the required raster format to determine slope. The default DEM resolution automatically suggested by the conversion tool in ESRI was about 6 m, but a more standard resolution of 5 m was chosen for the output DEM. The spot elevation points were also included in the conversion procedure to improve the accuracy of the resulting DEM.

4.3 Assessment and Preparation of Elevation Data

In preparation for analysis, the USGS DEMs needed to be in the same coordinate system as the pedestrian network. Before projecting the 1 m DEM, given that there were multiple 1 m DEM tiles needed to cover the study area, the 1 m DEM tiles were merged into one single, larger tile. The merged 1 m DEM and the other DEMs were then projected to the Pedestrian Network coordinate system. For the projections, bilinear interpolation was the resampling technique selected, keeping in mind ESRI's guidance that elevation is most appropriately resampled using bilinear interpolation (ESRI ArcGIS Help 10.2).

The original projected DEMs were much larger than the study area. To reduce the amount of time taken to render the DEM in the software application during analysis, all the DEMs (including the 5 m contour-derived DEM) were clipped to the same extent as the study area. Additionally, new lower resolution DEMs were created by resampling the clipped USGS 1 m DEM into 3 m, 5 m, and 10 m resolutions using bilinear interpolation. This enabled further comparisons between the lower resolution USGS DEMs and contour-derived DEM and the DEMs resampled from the high resolution 1 m DEM.

Once all the DEMs were processed, the minimum and maximum elevation values (about 109 m and 144 m, respectively) among all the DEMs, including the contour-derived DEM, were identified. These values were used when assigning minimum and maximum values to all of the DEMs for symbology purposes, so that the color ramps across all the DEMs would be consistent. Figure 12 shows the 1 m LiDAR-derived DEM, and Figure 13 shows the USGS 3 m DEM and the resampled 3 m DEM. The contour-derived 5 m DEM and the resampled 5 m DEM are shown in Figure 14, and lastly, Figure 15 shows the USGS 10 m DEM and the 10 m resampled DEM. While it is more difficult to visually identify differences between the 1 m and 3 m DEMs, differences can be observed in the 5 m DEMs, and the courser resolution of the 10 m DEMs is quite apparent.

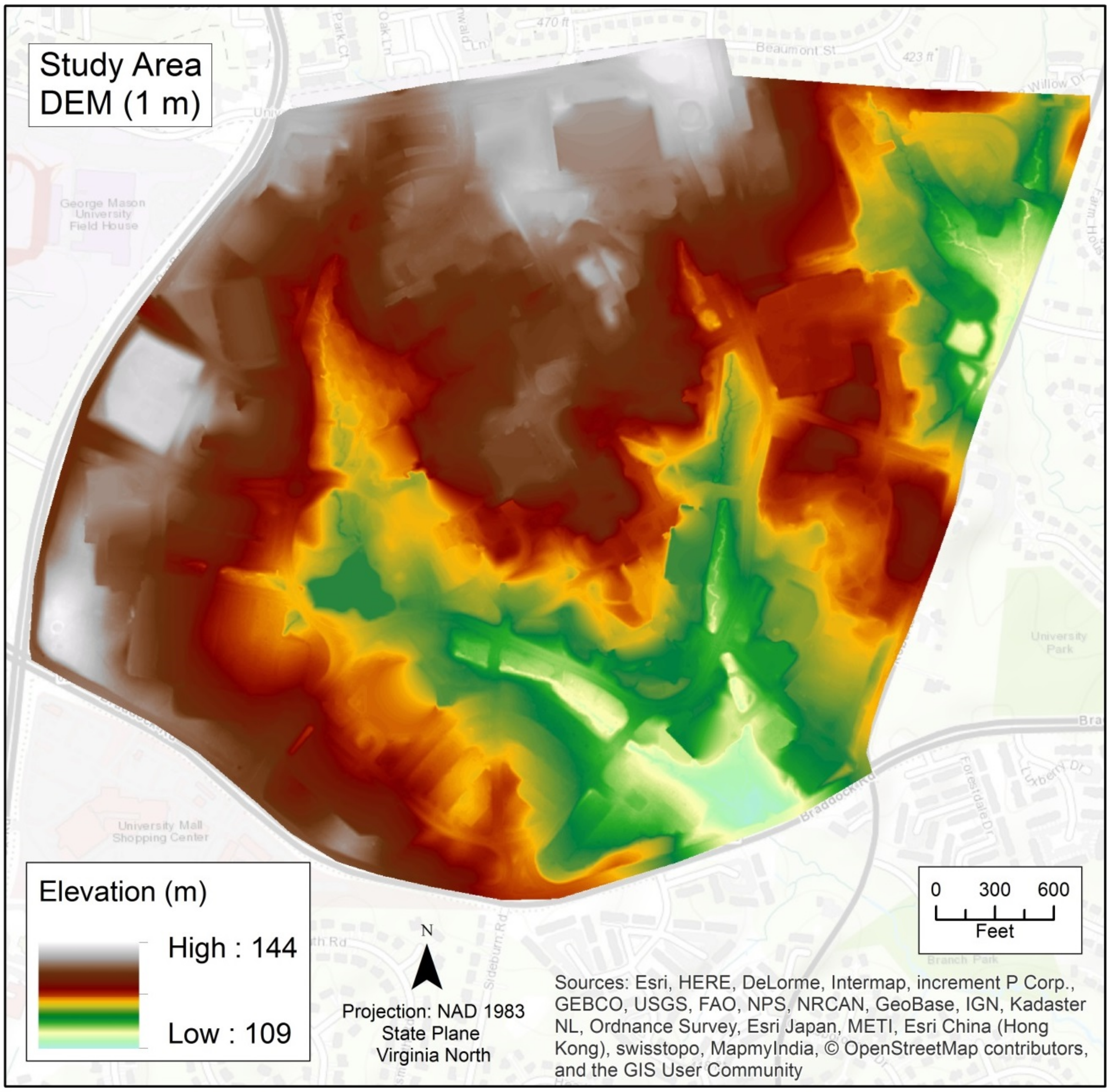

Figure 12 Study Area DEM: 1 m resolution

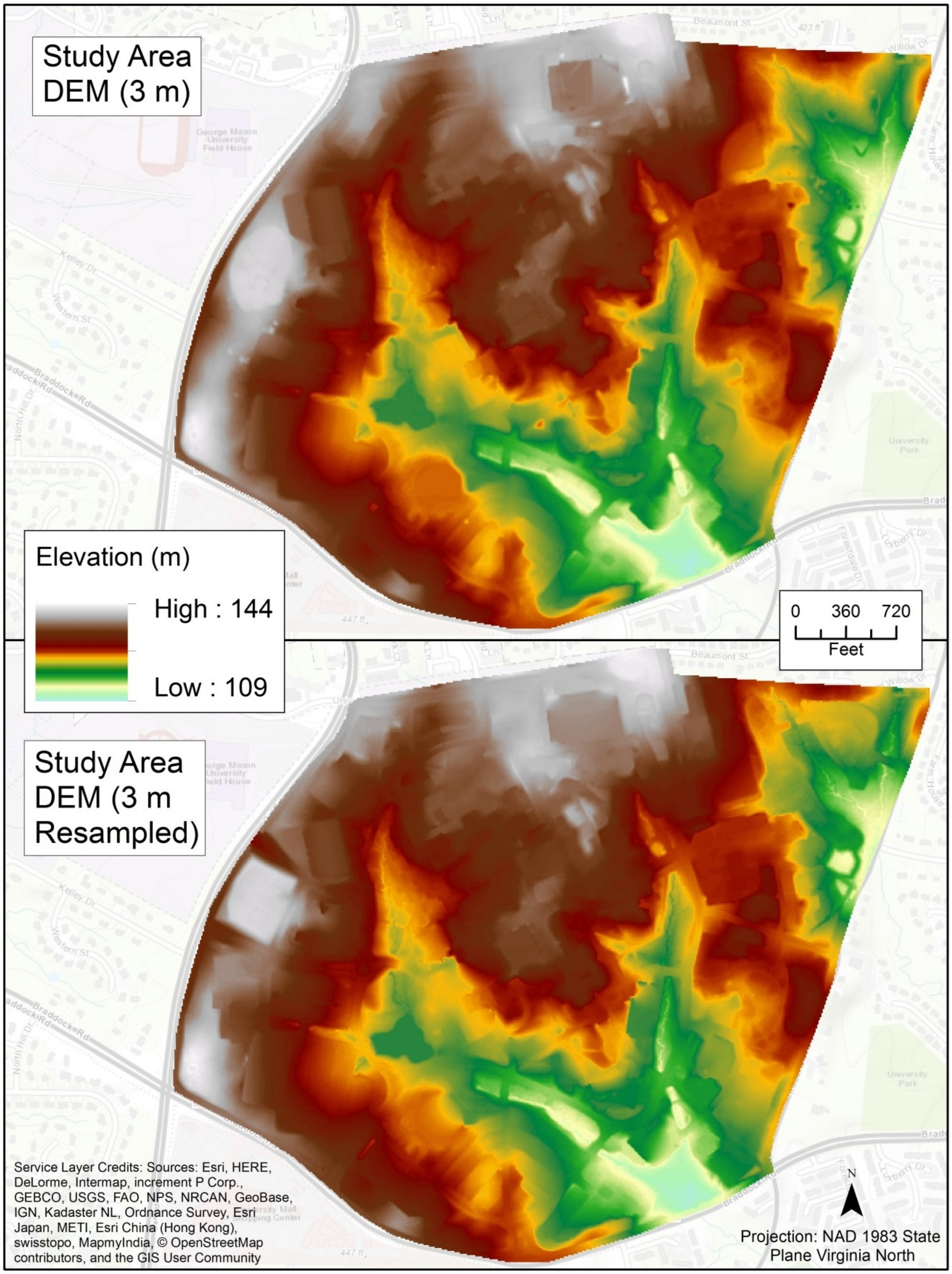

Figure 13 Study Area DEMs: 3 m resolution

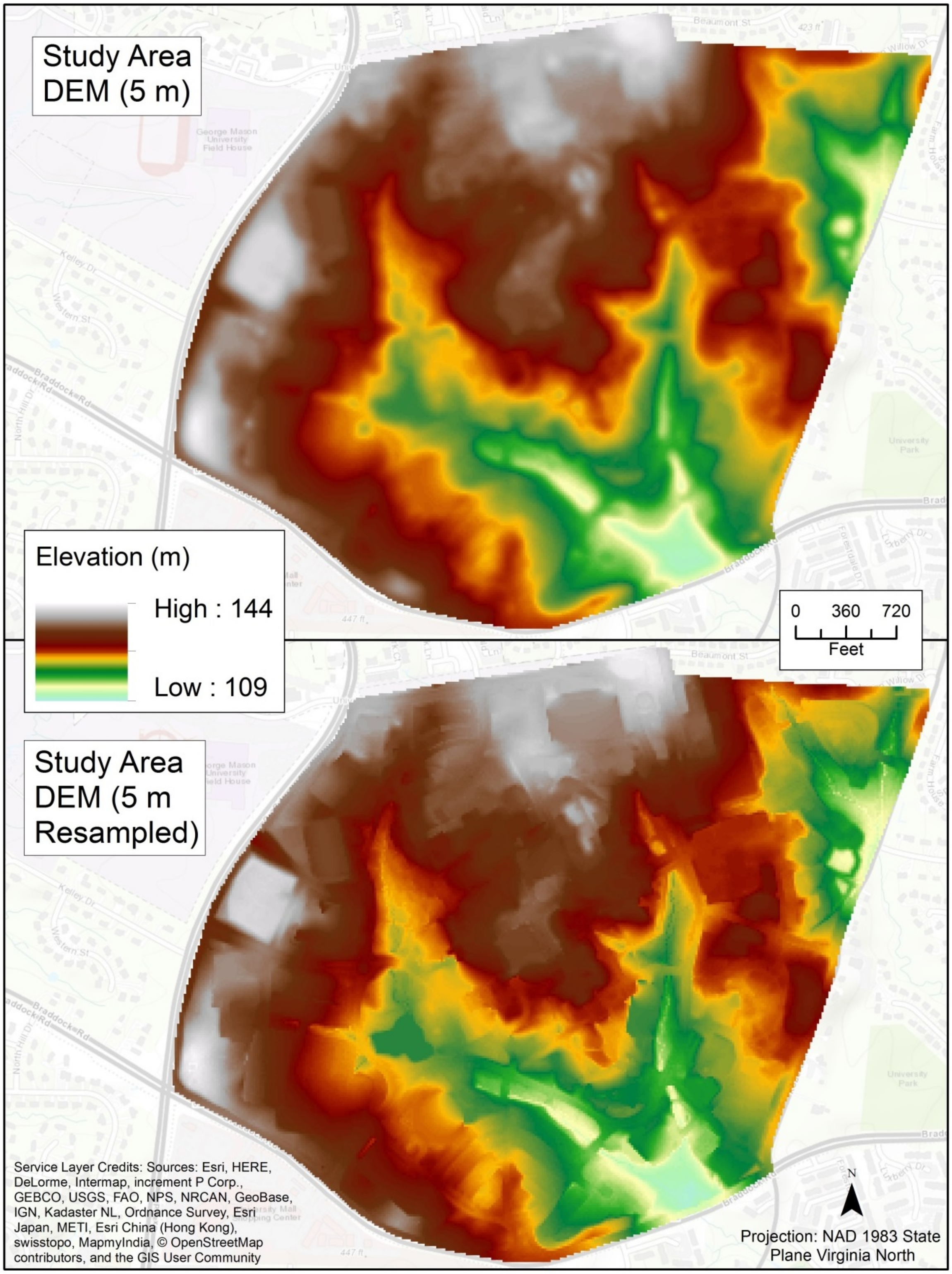

Figure 14 Study Area DEMs: 5 m resolution

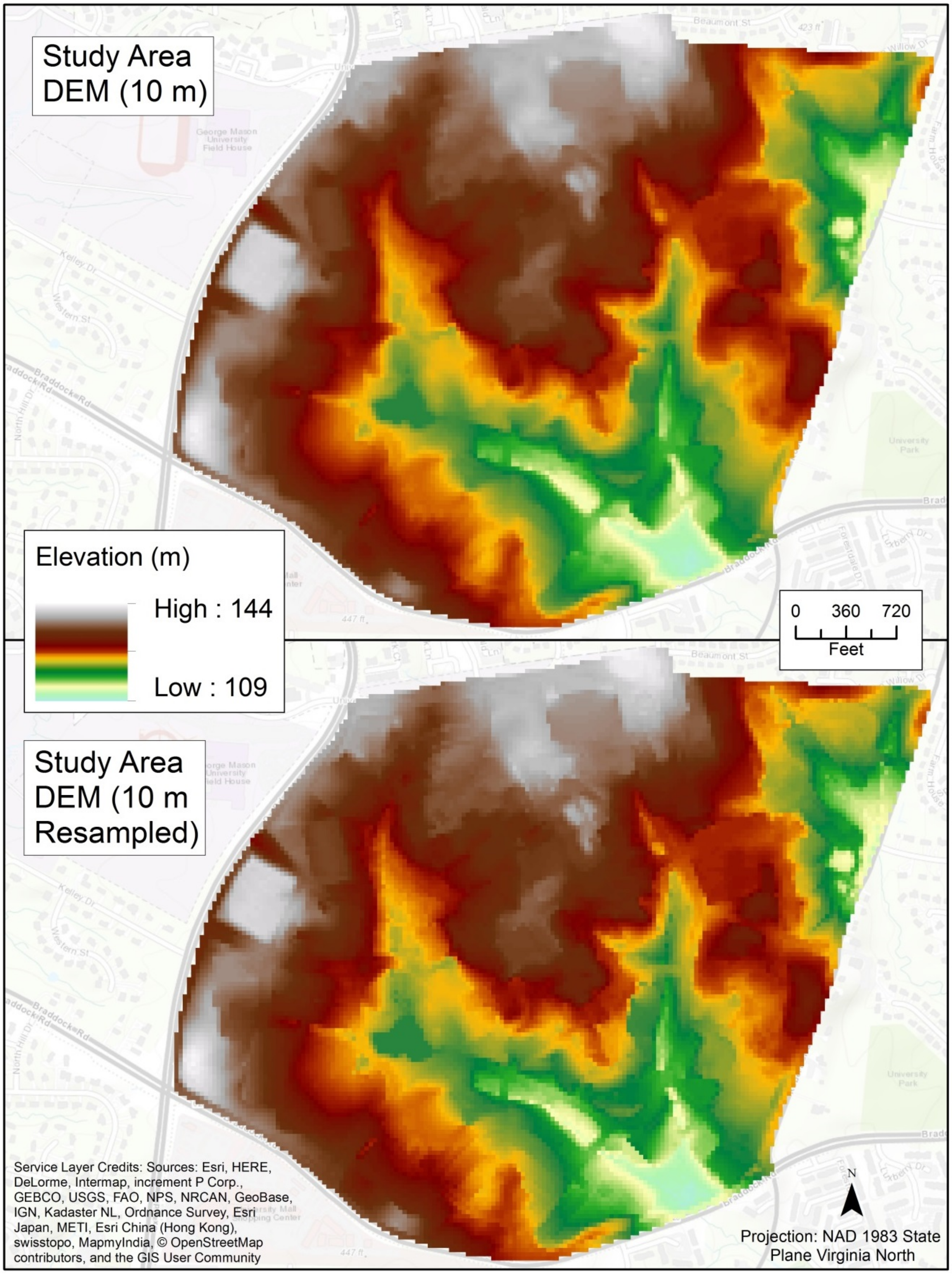

Figure 15 Study Area DEMs: 10 m resolution

4.4 Accuracy Assessment of DEMs

Given the conclusions drawn by James et al. (2006), Liu et al. (2007), and the Rutland Ranch Ground Truth survey sponsored by NOAA (2006) regarding the high level of accuracy of LiDAR data, it was decided that, due to the absence of ground truth sidewalk slope values over the study area, the 1 m LiDAR-derived DEM would serve as the "ground truth" dataset. Consequently, the slope values derived from the 1 m DEM were the standard to which the slope values from all the other elevation datasets were compared. In order to make the determination that the 1 m DEM was appropriate to use as the ground truth dataset, the RMSE between the field surveyed spot elevation points provided by GMU and the elevation values of those same points extracted from the 1 m DEM was calculated. It should be noted that, while it would not be correct to assume the spot elevations were error free, they could be considered to be an order of magnitude more accurate than the elevations provided by the DEMs.

When the elevations of the spot elevation points were extracted from the DEM, the elevation of the cell in which the point was located was calculated using bilinear interpolation, which takes adjacent cells into account. The RMSEs between the spot elevations and all the lower resolution DEMs were also calculated to verify that the smallest RMSE was indeed the one associated with the 1 m DEM. Smaller RMSEs indicate a better fit between the DEM and spot elevations. RMSE is calculated by taking the difference between the observed ground truth elevations (x_i) and the elevations in the DEM being compared to the ground truth (y_i). The differences in elevations are called residuals. The residuals for all the elevation points being compared are squared and then added together. This value is divided by the sample size (*n*), and finally, the square root of that value is taken to produce the RMSE. The formula is shown in Equation 1.

Equation 1 Calculation of Root Mean Square Error

$$\text{RMSE} = \sqrt{\frac{\sum_{i=1}^{n}(x_i - y_i)^2}{n}}$$

4.5 Calculation of Slope Values for Pedestrian Network

The importance of both slope and cross-slope has been discussed, and while cross-slope is a very important attribute to incorporate, this research focuses solely on the calculation of slope. When calculating slope, there are many different methods that can be used. Much research has been conducted to compare the accuracies of resulting slope values by using multiple slope calculation algorithms (Warren et al., 2004; Xuejun & Lu, 2008). One of the simplest approaches is, as in mathematics, to calculate the elevation change (rise) over a given distance (run). In this method, only the elevation values at the start and end points of any given line are used when calculating the slope. Elevation values for all start and end points of line features can be extracted from the DEMs and added as attributes in the Pedestrian Network. When the elevation values are extracted, the exact value of the cell in which the start/end point is located can be used, or the value can be interpolated, taking neighboring cells into account. The elevation values (represented as *z* in formulas) and positional (latitudinal and longitudinal) values (represented as *x* and *y*, respectively) of the start and end points can then be used to calculate the percent slope, as shown in Equation 2. This method does not take into account any variances in slope that may occur between the start and end points. The topographic profile in Figure 16 demonstrates this concept. If only the start and end points of the profile are used to calculate slope, significant slope variations in between the points are not captured. As such, it is better to use this method to calculate slope when the distance between start and end points is short.

Equation 2 Calculation of Percent Slope

$$\text{Percent Slope} = \frac{z_{end} - z_{start}}{\sqrt{(x_{start} - x_{end})^2 - (y_{start} - y_{end})^2}} \times \mathbf{100}$$

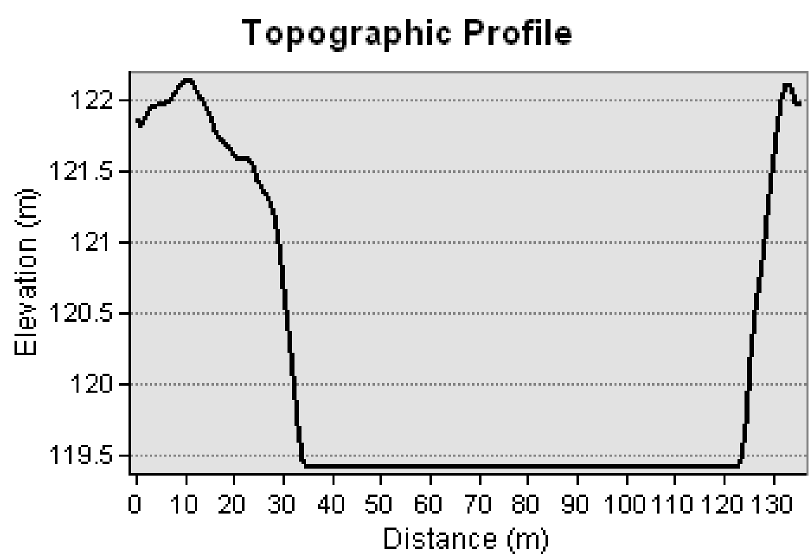

Figure 16 Variations in Slope Not Captured by Standard Slope Calculation

Another slope calculation approach is offered in ArcGIS: a tool called Add Surface Information. Any given line feature consists of a start point (also called a vertex) and an end point, but frequently, the line feature contains several more vertices in between the start and end points (Figure 17). This is the case with almost all, if not all, of the line features in the Pedestrian Network. The Add Surface Information tool calculates percent slope values for every segment between all the vertices for each line feature in the network. It obtains minimum slope from the segment whose value is closest to 0, or level (no slope). Maximum slope is obtained from the segment with the largest calculated slope value. Average slope is obtained by weighing each segment's slope by its 3D length, then determining the average. This results in longer segments having greater influence on the resulting slope value than shorter segments (ESRI ArcGIS Help 10.2). The segments in Figure 17 appear to have equal lengths, so they will equally influence the final slope value.

Figure 17 Single Line Feature with Multiple Vertices

In addition, the Add Surface Information tool uses the elevation values of the four nearest cells (versus only the cell in which the segment start or end vertex is located) to interpolate the elevation values of the segment vertices. While this method is also influenced by the overall length of the line features, the average slope value will be more accurate than the slope calculated by the standard method when there are notable slope variations within a line feature. Finally, one distinct advantage of this tool is that it requires less processing time by the analyst and is easy to implement.

For visualization purposes, seven copies of the Pedestrian Network were made so that each could contain slope information extracted from the USGS DEMs, the contour DEM, or the resampled DEMs. The Add Surface Information tool was run on the Pedestrian Network seven times, using each of the DEMs to extract minimum, maximum, and average elevation and percent slope values for all line features. These characteristics were automatically added as attribute fields in each Pedestrian Network copy. The interpolation method was bilinear, which is the only option available for raster datasets.

4.6 Statistical Analysis of Slope Values

In order to quantitatively determine whether or not DEM resolution had a significant influence on the slopes of the line features, differences in slope values between all possible DEM pairs were statistically assessed. Slopes from the resampled 3 m, 5 m, and 10 m DEMs, the USGS 3 m and 10 m DEMs, and the contour-derived 5 m DEM were all compared with slopes from the USGS 1 m DEM. The slopes from the lower resolution DEMs were also compared with one another, so that conclusions could be drawn regarding the utility of one with respect to the other. For example, if the slope differences between the 3 m DEM and the 5 m DEM were not statistically significant, then it could be concluded that the DEMs were equally useful for determining slope for the selected study area.

Before statistical tests could be performed, the slope differences between all DEM pairs first needed to be tested for normality. While parametric statistical tests assume a normal, Gaussian distribution of observations, nonparametric tests do not make that assumption. In this analysis, only differences were tested for normality (as opposed to the original slope values of both datasets being compared), because it is the distribution of the differences that has to be normal for parametric tests (Mordkoff, 2011). To test for normality, a suite of statistics tools called StatPlus was used. Its normality tests include the following: the Kolmogorov-Smirnov/Lilliefor test; the Shapiro-Wilk W test; the D'Agostino Skewness test; the D'Agostino Kurtosis test; and the D'Agostino Omnibus test. By default, all the tests are performed on the input data. Advanced options are available that allow the alpha value for the desired confidence interval to be specified. The normality tests were run on the differences for all DEM pairs, and an alpha value of 5% (0.05) was specified.

If the distribution of the differences were normal, then the paired *t*-test would be the appropriate parametric statistical test to use. In fact, several similar studies (Warren et al., 2004; Weih & Mattson, 2004; White, Dietterick, Mastin, & Strohman, 2010) assessed slope accuracy using the paired *t*-test. A paired *t*-test is used to compare two population means, where there are two samples in which observations in one sample can be paired with observations in the other sample. This was applicable in this situation because every pair of slopes being compared was for the same line feature. However, if the results of the normality tests showed that the slope differences did not have a normal distribution, a nonparametric test would need to be employed. The nonparametric test that is the counterpart of the paired *t*-test is called the Wilcoxon signed-rank test, which has also been used to assess differences in slope values (Thompson, Bell, & Butler, 2001). The Wilcoxon signed-rank test also compares two paired samples, but it does not require the normality of within-pair differences, as the paired *t*-test does. Also, it compares the medians of two populations, as opposed to means in the paired *t*-test.

Parametric tests are usually more powerful than their nonparametric counterparts. Consequently, if it is possible to justify the assumptions of a parametric test, that is the preferable course of action (McCrum-Gardner, 2008). If the normality assumption is not met in this case, it may still be reasonable to justify using the paired *t*-test. Mordkoff (2011) explains that Central Limit Theorem states that, "given random and independent samples of *N* observations each, the distribution of sample means approaches normality as the size of *N* increases, regardless of the shape of the population distribution" (p. 2). For this reason, referring specifically to the paired *t*-test, Samuels, Witmer, & Schaffner (2012) also suggest that a widely accepted exception to the normality assumption for the paired *t*-test is that the test is also valid if the sample size is large. A sample is considered large if the number of observations is greater than or equal to 30.

To be thorough and to observe whether or not discrepancies would arise, both parametric and nonparametric tests were conducted. Two-tailed paired *t*-tests and two-tailed Wilcoxon signed-rank tests were performed between all pairs of DEMs using the Real Statistics Resource Pack, a free statistical analysis toolset for Microsoft Excel. Two-tailed tests were performed because it was anticipated that there could be negative and positive differences for slope values between two datasets. For the paired *t*-tests, the null hypothesis was that the mean difference between pairs of observations would be zero; for the Wilcoxon tests, the null hypothesis was that the median difference between pairs would be zero. For all tests, the alpha value was set to 5% (0.05), and the sample size was 2,887.

The paired *t*-test's null hypothesis is rejected or fails to be rejected depending on the relationship between the *t* statistic (t) and the critical value of the *t* statistic (t_{crit}); the Wilcoxon test's null hypothesis is rejected or fails to be rejected depending on the relationship between the T statistic (T) and the critical value of the T statistic (T_{crit}). All of these values are provided as outputs of the tests. The alpha value is taken into account by t_{crit} /T_{crit}. The null hypothesis fails to be rejected (in other words, it is true) for the paired *t*-test if t_{crit} is greater than t; for the Wilcoxon test, it is when T is greater than T_{crit} that the null hypothesis fails to be rejected.

CHAPTER FIVE

5.1 DEM Accuracy Results

The accuracy assessment of the elevations extracted from the 1 m LiDAR-derived DEM provided an RMSE of 0.3 m, or 1 foot. Upon closer inspection, it was determined that 88% of the 1 m DEM elevation points had differences of 0.3 m (1 foot) or less when compared to the field surveyed spot elevation points. Since time and resources were not available to collect sufficient ground truth slope measurements for this research, it was determined that it was reasonable to use the 1 m DEM as the ground truth DEM. Table 2 displays summary statistics and the RMSE for the differences between the spot elevations and the 1 m DEM, in addition to the other DEMs used in the analysis, to demonstrate that the 1 m DEM does in fact have the smallest RMSE. Table 3 includes the summary statistics and RMSEs for the DEMs resampled from the 1 m DEM. In all cases, the total number of points (sample size) was 3,066.

Table 2 Summary Statistics: DEM and Spot Elevation Differences (meters)

DEM	Maximum	Minimum	Mean	Standard Deviation	RMSE
1 m	3.249	-2.515	0.175	0.256	0.310
3 m	4.040	0.218	0.082	0.706	0.710
5 m	2.074	0.053	-0.002	0.381	0.381
10 m	3.829	0.212	0.157	0.362	0.394

Table 3 Summary Statistics: Resampled DEM and Spot Elevation Differences (meters)

DEM	Maximum	Minimum	Mean	Standard Deviation	RMSE
3 m	3.300	0.196	0.171	0.263	0.313
5 m	3.117	0.270	0.170	0.275	0.323
10 m	3.762	0.267	0.161	0.326	0.363

5.2 Slope Results

The total number of sidewalk line features for which percent slope values were calculated across all DEMs was 2,887. Since the GMU testbed routing environment is concerned with steep slopes that would be an impediment for disabled pedestrians, it is worthwhile to look at the maximum slope in addition to the average slope along any given line. Tables 4 and 5 provide summary statistics for the average and maximum (respectively) percent slope values derived from each of the DEMs. DEMs resampled from the 1 m DEM have an (R) beside them. The summary statistics demonstrate that there are variations present in the slopes of some line features that result in maximum slope being noticeably greater than average slope.

Table 4 Summary Statistics: Average Percent Slope

DEM	Minimum	Maximum	Mean	Standard Deviation
1 m	0.088	12.363	1.238	1.255
3 m	0.047	12.442	1.282	1.153
3 m (R)	0.041	11.760	1.212	1.172
5 m	0.023	6.247	1.074	0.814
5 m (R)	0.013	11.211	1.218	1.112
10 m	0.015	9.705	1.122	0.940
10 m (R)	0.016	11.149	1.179	0.985

Table 5 Summary Statistics: Maximum Percent Slope

DEM	Minimum	Maximum	Mean	Standard Deviation
1 m	0.152	38.016	2.616	2.833
3 m	0.081	24.632	2.332	2.040
3 m (R)	0.097	39.832	2.302	2.259
5 m	0.042	6.842	1.473	0.921
5 m (R)	0.014	23.457	2.241	1.962
10 m	0.018	15.650	1.729	1.337
10 m (R)	0.044	15.172	1.989	1.555

To facilitate the visualization of the differences in slope results derived from each DEM, the Pedestrian Network sidewalk lines were assigned various colors representing the categories to which each line feature belonged, based on slope. The categories included: Level (0 – 2%); Very Gentle Slope (>2 – 5%); Gentle Slope (>5% – 8.33%); Moderate Slope (>8.33 – 15%); and Strong Slope (>15%). Categories were identified by referencing a standard slope descriptors table (Barcelona Field Studies Centre, 2013) and taking ADA guidelines into account. Maximum, versus average (running), slope was selected as the attribute to display. Even if a sidewalk were classified as having a percent average slope in the Gentle Slope category and could likely be manageable for a disabled pedestrian over short distances, if there were a section of the sidewalk that had steeper slope (which would be captured as maximum percent slope), the pedestrian would be at a disadvantage and would probably have to turn around and find an alternate route. Table 6 shows the number of line features in each maximum slope category for all the DEMs. Figures 18 through 21 display the Pedestrian Network sidewalk slopes, categorized by percent maximum slope, that resulted from using varying DEM resolutions to extract slope information.

Table 6 Line Features in Each Maximum Slope Category by DEM

DEM	Level (0 - 2%)	Very Gentle (>2 - 5%)	Gentle (>5 – 8.33%)	Moderate (>8.33 – 15%)	Strong (>15%)	Total
1 m	1647	944	136	140	20	2887
3 m	1679	964	188	48	8	2887
3 m (R)	1763	879	172	64	9	2887
5 m	2224	655	8	0	0	2887
5 m (R)	1739	936	160	46	6	2887
10 m	2024	781	73	8	1	2887
10 m (R)	1823	929	113	21	1	2887

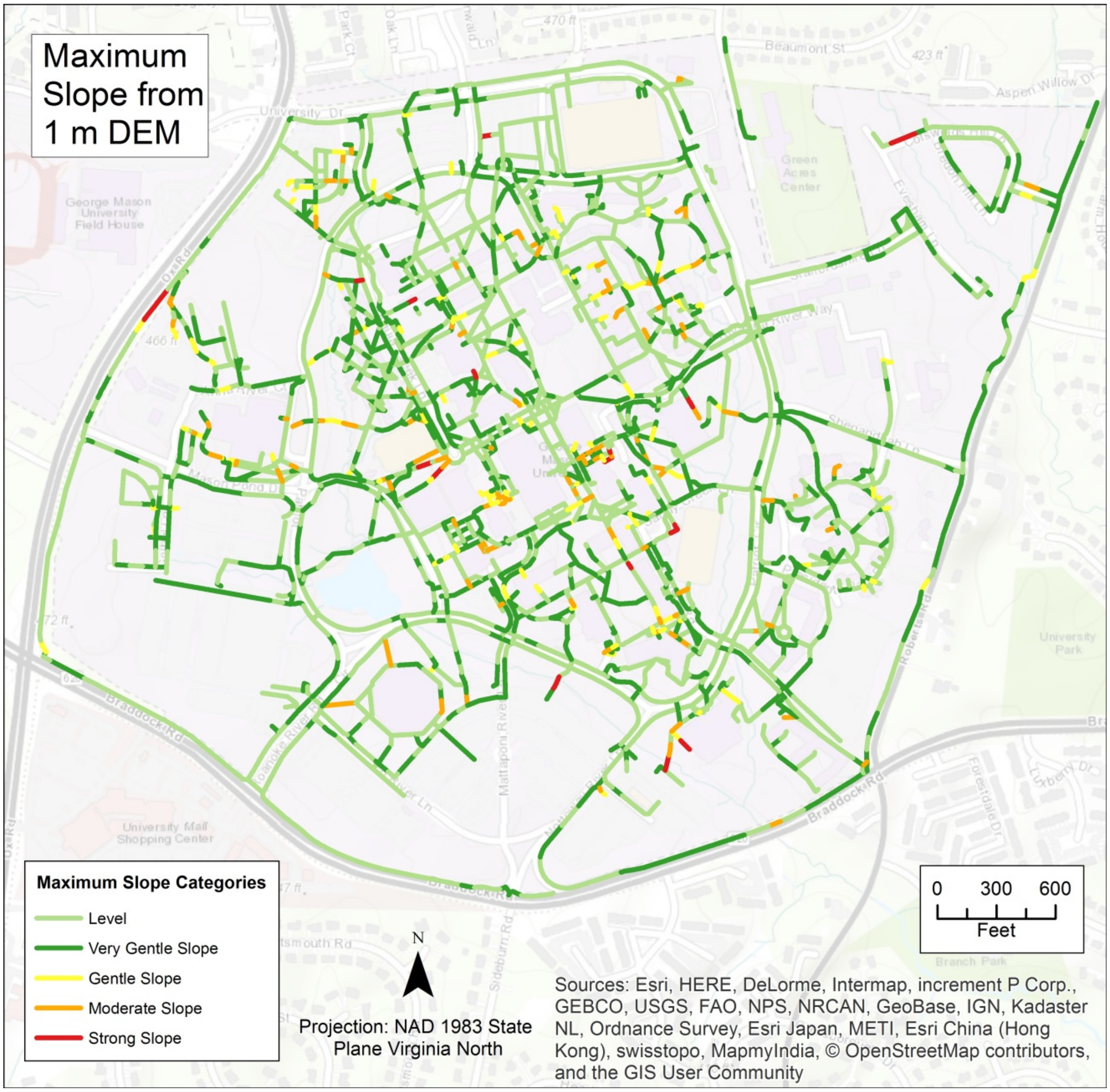

Figure 18 Percent Maximum Slope Results: 1 m DEM

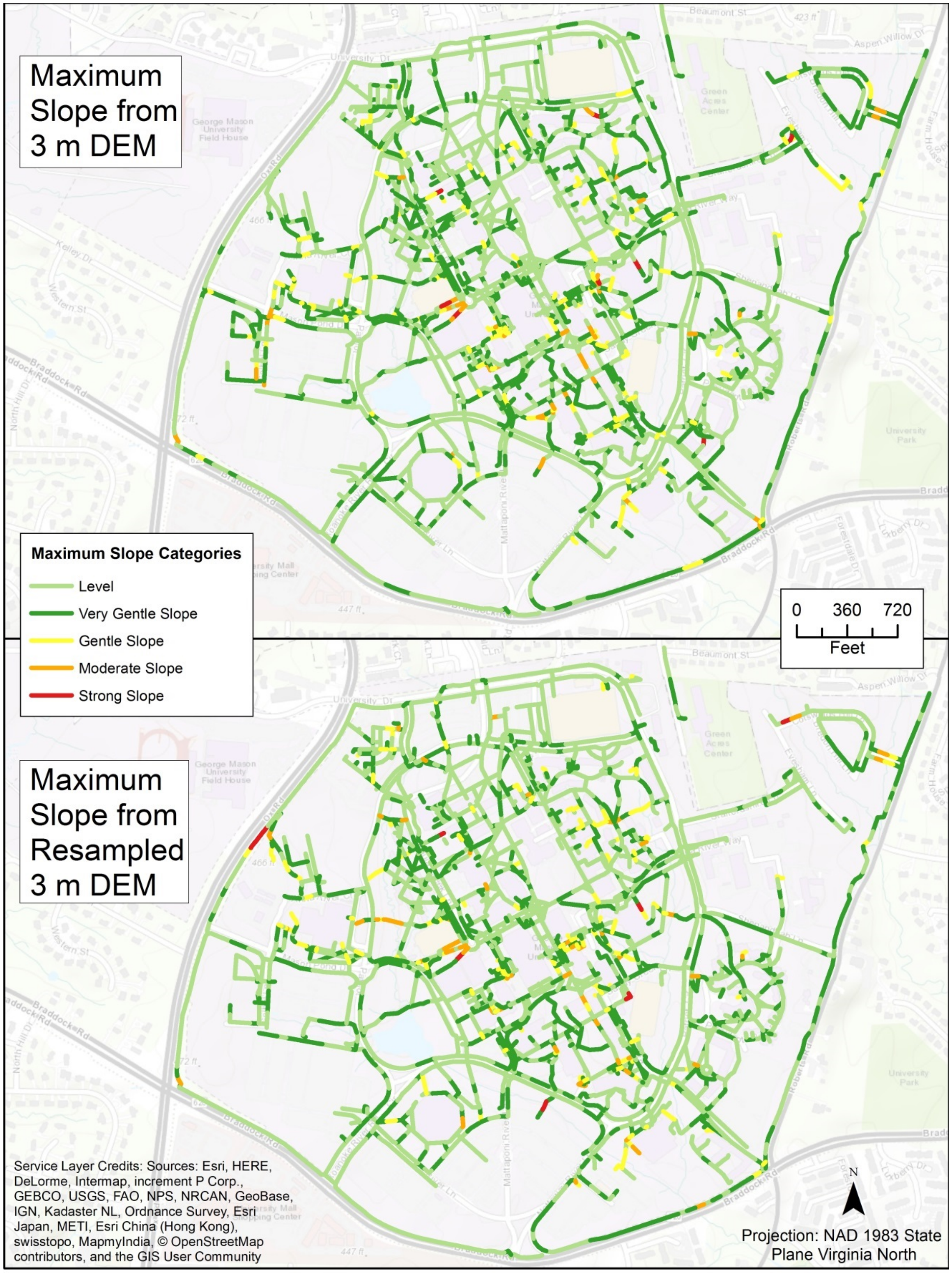

Figure 19 Percent Maximum Slope Results: 3 m DEM and Resampled 3 m DEM

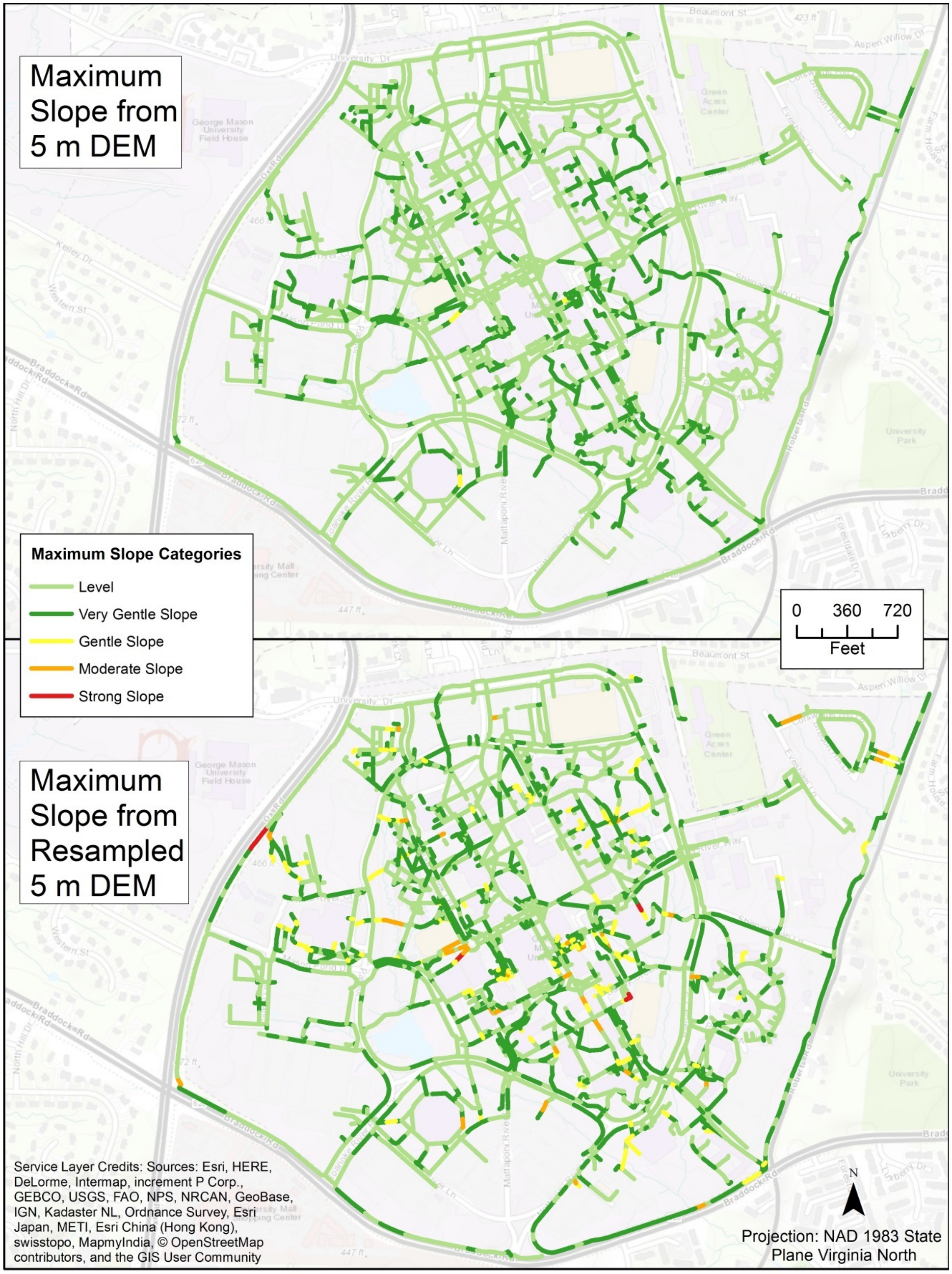

Figure 20 Percent Maximum Slope Results: 5 m DEM and Resampled 5 m DEM

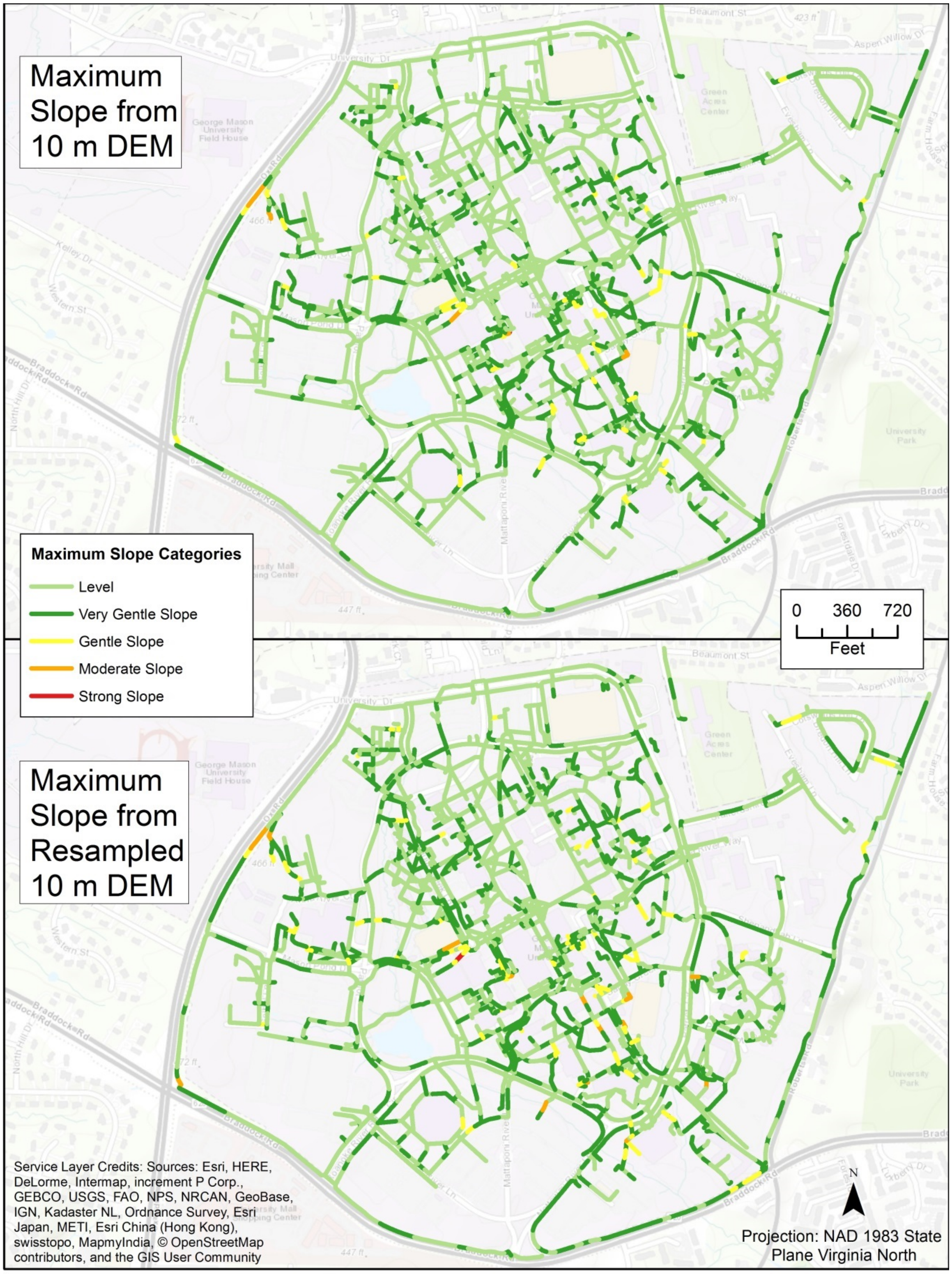

Figure 21 Percent Maximum Slope Results: 10 m DEM and Resampled 10 m DEM

5.3 Statistical Analysis Results

The results of the normality tests consistently concluded that the distributions of all the paired DEM differences were not normal. Figures 22, 23, and 24 display the results of the Kolmogorov-Smirnov/Lilliefor, Shapiro-Wilk W, D'Agostino Skewness, D'Agostino Kurtosis, and D'Agostino Omnibus normality tests performed on each pair. In all cases, the p-level is less than alpha (5%, or 0.05), leading to the conclusion that the null hypothesis—that the distributions are normal—should be rejected. The figures also show the histograms for each pair comparison so that the actual distributions can be visualized. The red line on the histograms represents the normal curve of the distribution.

The results of the paired *t*-tests and Wilcoxon signed-rank tests are displayed in Table 7. No discrepancies arose between the results of the two tests; if the paired *t*-test rejected the null hypothesis, the Wilcoxon signed-rank test also rejected the null hypothesis. For the 12 comparisons made between DEM pairs, 11 suggested that the differences between the DEM pairs were statistically significant. This could be concluded for the paired *t*-tests because t_{crit} was less than t. For the Wilcoxon signed-rank tests, this conclusion was drawn because T was less than T_{crit}. For both tests, the fact that the p-value was less than alpha (0.05) led to the rejection of the null hypothesis (that the mean [for paired *t*-tests] or median [for Wilcoxon signed-rank tests] difference between pairs of observations was zero).

The only pair for which the tests suggested that there was no statistically significant difference was the 3 m DEM and 3 m resampled DEM pair. In that case, t was less than t_{crit} for the paired *t*-test, and T_{crit} was less than T for the Wilcoxon signed-rank test. Additionally, the p-values of both tests were greater than alpha (0.05), meaning that the null hypothesis failed to be rejected.

It can be observed that, for some of the paired *t*-tests, the value of the t-statistic, *t*, is negative. The negative value simply conveys the direction of the difference in the means, and this is why a two-tail *t*-test was conducted. In these situations, when comparing t with t_{crit}, the absolute value of t is used (Elrod, 2015).

Normality Test	Test Statistics	p-level	Conclusion (5%)
Kolmogorov-Smirnov/Lilliefor Test	0.2114	0.00	*Strong evidence against normality*
Shapiro-Wilk W	0.7388	0.00	*Reject Normality*
D'Agostino Skewness	29.4819	0.00	*Reject Normality*
D'Agostino Kurtosis	27.9158	0.00	*Reject Normality*
D'Agostino Omnibus	1,648.4748	0.00	*Reject Normality*

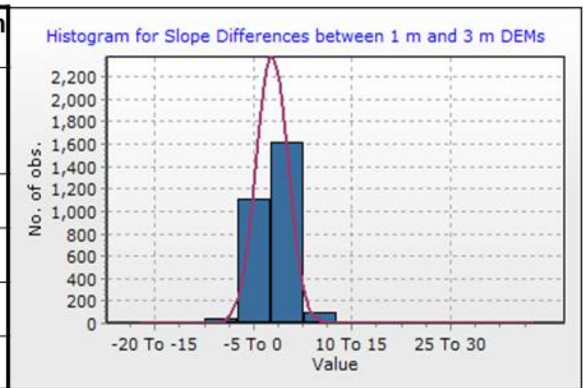

Normality Test	Test Statistics	p-level	Conclusion (5%)
Kolmogorov-Smirnov/Lilliefor Test	0.2097	0.00	*Strong evidence against normality*
Shapiro-Wilk W	0.7346	0.00	*Reject Normality*
D'Agostino Skewness	30.2288	0.00	*Reject Normality*
D'Agostino Kurtosis	25.1433	0.00	*Reject Normality*
D'Agostino Omnibus	1,545.9644	0.00	*Reject Normality*

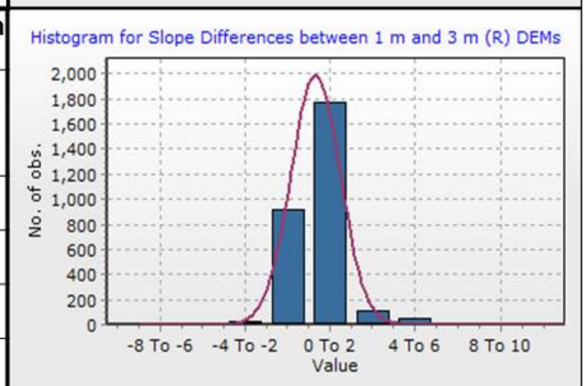

Normality Test	Test Statistics	p-level	Conclusion (5%)
Kolmogorov-Smirnov/Lilliefor Test	0.263	0.00	*Strong evidence against normality*
Shapiro-Wilk W	0.6058	0.00	*Reject Normality*
D'Agostino Skewness	42.274	0.00	*Reject Normality*
D'Agostino Kurtosis	28.92	0.00	*Reject Normality*
D'Agostino Omnibus	2,623.4566	0.00	*Reject Normality*

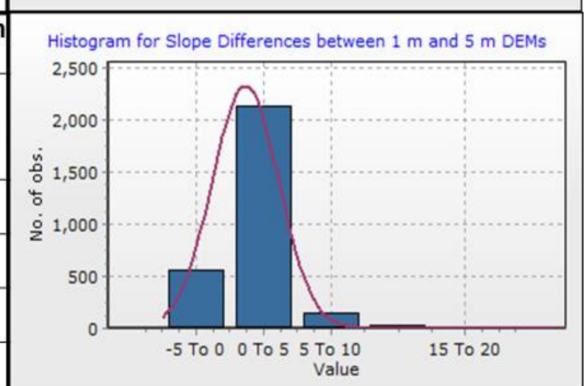

Normality Test	Test Statistics	p-level	Conclusion (5%)
Kolmogorov-Smirnov/Lilliefor Test	0.2126	0.00	*Strong evidence against normality*
Shapiro-Wilk W	0.7222	0.00	*Reject Normality*
D'Agostino Skewness	35.7995	0.00	*Reject Normality*
D'Agostino Kurtosis	27.8697	0.00	*Reject Normality*
D'Agostino Omnibus	2,058.3273	0.00	*Reject Normality*

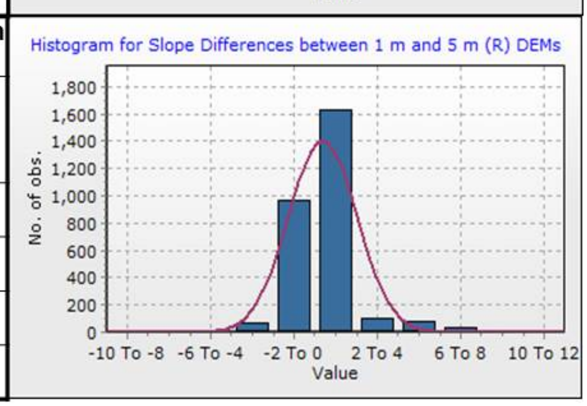

Figure 22 Normality Test Results, Part 1

Normality Test	Test Statistics	p-level	Conclusion (5%)
Kolmogorov-Smirnov/Lilliefor Test	0.2409	0.00	*Strong evidence against normality*
Shapiro-Wilk W	0.67	0.00	*Reject Normality*
D'Agostino Skewness	38.3628	0.00	*Reject Normality*
D'Agostino Kurtosis	26.9138	0.00	*Reject Normality*
D'Agostino Omnibus	2,196.0563	0.00	*Reject Normality*

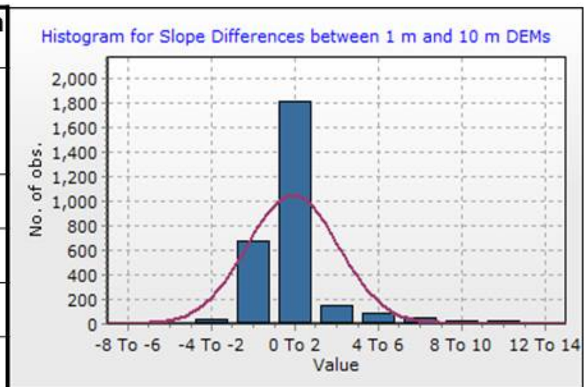

Normality Test	Test Statistics	p-level	Conclusion (5%)
Kolmogorov-Smirnov/Lilliefor Test	0.2287	0.00	*Strong evidence against normality*
Shapiro-Wilk W	0.7202	0.00	*Reject Normality*
D'Agostino Skewness	36.0285	0.00	*Reject Normality*
D'Agostino Kurtosis	26.147	0.00	*Reject Normality*
D'Agostino Omnibus	1,981.7173	0.00	*Reject Normality*

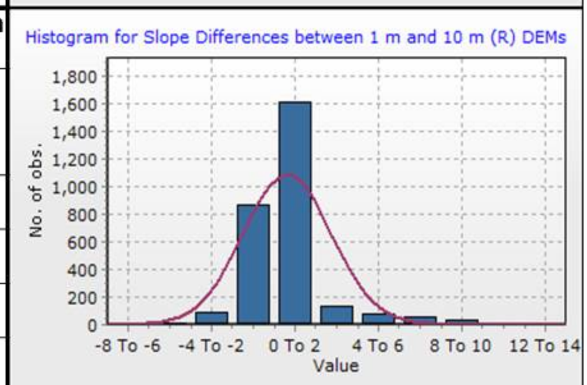

Normality Test	Test Statistics	p-level	Conclusion (5%)
Kolmogorov-Smirnov/Lilliefor Test	0.1794	0.00	*Strong evidence against normality*
Shapiro-Wilk W	0.7357	0.00	*Reject Normality*
D'Agostino Skewness	26.5233	0.00	*Reject Normality*
D'Agostino Kurtosis	31.0835	0.00	*Reject Normality*
D'Agostino Omnibus	1,669.6712	0.00	*Reject Normality*

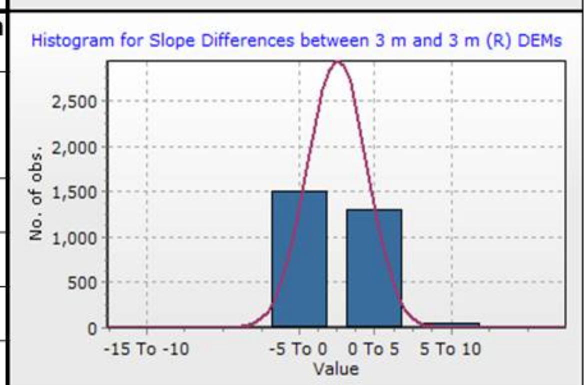

Normality Test	Test Statistics	p-level	Conclusion (5%)
Kolmogorov-Smirnov/Lilliefor Test	0.1861	0.00	*Strong evidence against normality*
Shapiro-Wilk W	0.7266	0.00	*Reject Normality*
D'Agostino Skewness	38.1272	0.00	*Reject Normality*
D'Agostino Kurtosis	26.7817	0.00	*Reject Normality*
D'Agostino Omnibus	2,170.9435	0.00	*Reject Normality*

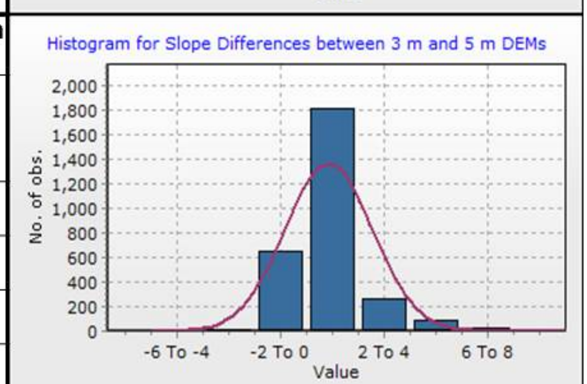

Figure 23 Normality Test Results, Part 2

Normality Test	Test Statistics	p-level	Conclusion (5%)
Kolmogorov-Smirnov/Lilliefor Test	0.1744	0.00	*Strong evidence against normality*
Shapiro-Wilk W	0.7687	0.00	*Reject Normality*
D'Agostino Skewness	28.9362	0.00	*Reject Normality*
D'Agostino Kurtosis	26.1113	0.00	*Reject Normality*
D'Agostino Omnibus	1,519.1039	0.00	*Reject Normality*

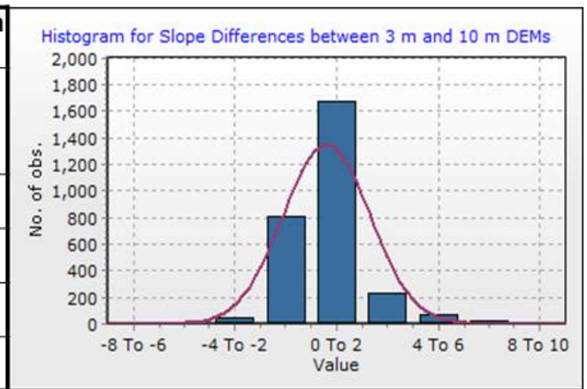

Normality Test	Test Statistics	p-level	Conclusion (5%)
Kolmogorov-Smirnov/Lilliefor Test	0.1658	0.00	*Strong evidence against normality*
Shapiro-Wilk W	0.726	0.00	*Reject Normality*
D'Agostino Skewness	41.8869	0.00	*Reject Normality*
D'Agostino Kurtosis	29.568	0.00	*Reject Normality*
D'Agostino Omnibus	2,628.7803	0.00	*Reject Normality*

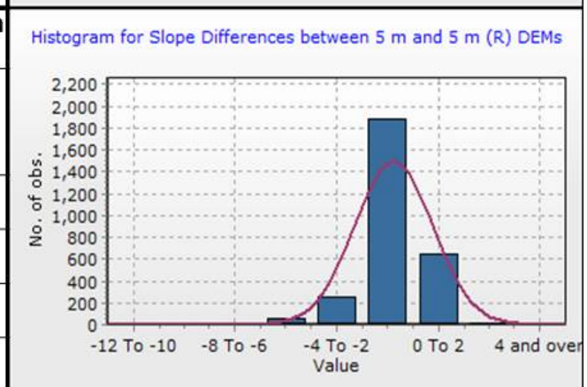

Normality Test	Test Statistics	p-level	Conclusion (5%)
Kolmogorov-Smirnov/Lilliefor Test	0.1468	0.00	*Strong evidence against normality*
Shapiro-Wilk W	0.7525	0.00	*Reject Normality*
D'Agostino Skewness	41.8101	0.00	*Reject Normality*
D'Agostino Kurtosis	30.2355	0.00	*Reject Normality*
D'Agostino Omnibus	2,662.2734	0.00	*Reject Normality*

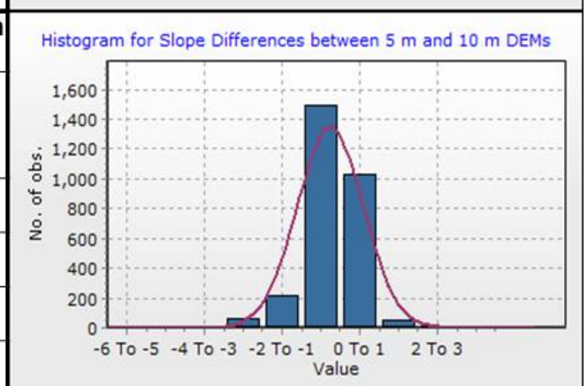

Normality Test	Test Statistics	p-level	Conclusion (5%)
Kolmogorov-Smirnov/Lilliefor Test	0.1208	0.00	*Strong evidence against normality*
Shapiro-Wilk W	0.8663	0.00	*Reject Normality*
D'Agostino Skewness	12.91	0.00	*Reject Normality*
D'Agostino Kurtosis	23.583	0.00	*Reject Normality*
D'Agostino Omnibus	722.8246	0.00	*Reject Normality*

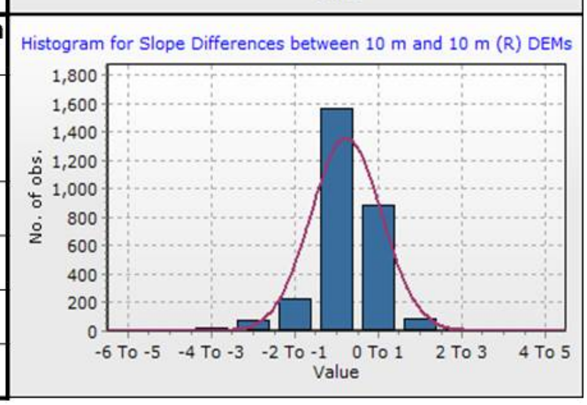

Figure 24 Normality Test Results, Part 3

Table 7 Paired *t*-Test and Wilcoxon Signed-Rank Test Results

Pair	Summary of Differences			Paired *t*-Test (Two Tail)					Wilcoxon Signed-Rank Test (Two Tail)			
	Mean	*Std Dev*	*Std Error*	*deg. freedom*	*t*	t_{crit}	*p-value*	*sig*	*T*	T_{crit}	*p-value*	*sig*
1m - 3m	0.284	2.411	0.045	2886	6.327	1.961	0.000	yes	1,678,485	1,996,624	0.000	yes
1m - 3m (R)	0.314	1.158	0.022	2886	14.574	1.961	0.000	yes	1,242,063	1,996,624	0.000	yes
1m - 5m	1.143	2.475	0.046	2886	24.824	1.961	0.000	yes	579,931	1,996,624	0.000	yes
1m - 5m (R)	0.375	1.641	0.031	2886	12.289	1.961	0.000	yes	1,440,695	1,996,624	0.000	yes
1m - 10m	0.888	2.197	0.041	2886	21.708	1.961	0.000	yes	844,688	1,996,624	0.000	yes
1m - 10m (R)	0.628	2.131	0.040	2886	15.826	1.961	0.000	yes	1,303,715	1,996,624	0.000	yes
3m - 3m (R)	0.030	1.928	0.036	2886	0.845	1.961	0.398	no	2,013,256	1,996,624	0.112	no
3m - 5m	0.859	1.692	0.031	2886	27.295	1.961	0.000	yes	670,923	1,996,624	0.000	yes
3m - 10m	0.604	1.702	0.032	2886	19.064	1.961	0.000	yes	1,040,563	1,996,624	0.000	yes
5m - 5m (R)	-0.768	1.546	0.029	2886	-26.689	1.961	0.000	yes	654,247	1,996,624	0.000	yes
5m - 10m	-0.256	0.855	0.016	2886	-16.059	1.961	0.000	yes	1,307,072	1,996,624	0.000	yes
10m - 10m (R)	-0.260	0.846	0.016	2886	-16.527	1.961	0.000	yes	1,209,605	1,996,624	0.000	yes

The sample size, or number of observations, is 2,887. Alpha is 0.05. Summary of Differences units are (maximum) percent slope.

5.4 Discussion

As expected, the RMSEs between the field surveyed spot elevations and the 3 m, 5 m, and 10 m DEMs were greater than the RMSE associated with the 1 m DEM. Since the RMSE conveys how well the DEM elevation values match the spot elevations, and lower RSMEs indicate a better fit, it is not surprising that the lowest RMSE is associated with the highest resolution DEM. It was unusual, however, that the RMSE of the 3 m DEM was higher than the RMSEs of the 5 m and 10 m. The expected pattern would be for the RMSEs to increase with lower DEM resolutions, and this was the case with all the DEMs, including the resampled versions, aside from the 3 m DEM. This discrepancy may be due to the fact that the 3 m DEM is older (from 2008) and may have had more errors present that were not corrected. The USGS corrects DEM errors encountered as new datasets are acquired, but given the production of 1 m DEMs as part of the 3DEP, the 3 m DEMs will no longer be updated. When comparing the resampled DEMs with the lower resolution USGS and contour-derived DEM, it was observed that, for the same resolutions, the resampled DEMs had lower RMSEs. This observation corroborates the conclusions drawn by Vaze et al. (2010) that, when a lower resolution DEM is needed based on the scale of a study, it is better to resample an available higher resolution DEM than to use the original lower resolution DEM.

In conjunction with Table 7, Figures 18 through 21 display the differences present in the number of line features in each slope category among all the DEMs considered. The majority of line features are in the Level slope category, regardless of DEM resolution. As DEM resolution becomes coarser, fewer and fewer line features are placed in the higher maximum slope categories, such as Moderate and Strong. In the figures, this is made apparent by the Pedestrian Network becoming more and more dominated by the light green (Level) and green (Very Gentle) color categories. In fact, the 5 m DEM derived from the campus contours does not have any line features classified as Moderate or Strong. It contains almost all light green and green line features, as opposed to its resampled 5 m counterpart, which displays more variation. This was likely due to the fact that a certain degree of detail was not captured by the DEM created from the contour lines, since the areas between the contour lines were interpolated. In general, as terrain surface detail is gradually reduced by moving from higher to lower resolution DEMs, it produces a smoothing effect (Weih & Mattson, 2004; Gillin, Bailey, McGuire, & Prisley, 2015). It can be more readily understood when described as follows: one single 10 m by 10 m cell covers the same area that is covered by one hundered 1 m by 1 m cells. The one hundred cells can capture variations in elevation values, whereas the single 10 m cell has only one elevation value to represent the entire area. Although it was anticipated that the 10 m DEM would likely not capture the level of slope detail needed for accessible routing for this study area, it was included to demonstrate and facilitate an understanding of how detail is lost by lowering the resolution.

The visual assessment of the Pedestrian Network classified by color-coded maximum percent slope categories, along with the corresponding table (Table 6), was sufficient to be able to qualitatively convey that the lower resolution DEMs did not capture the slope variations of the sidewalk line features as well as the 1 m DEM. However, it was preferred that this observation also be assessed using quantitative methods, so that the final conclusions could be made with more objective information regarding the differences in the slopes captured by the various DEMs. The DEMs were therefore compared statistically to detect significant differences. It was initially decided that the parametric paired *t*-test was the appropriate test to use for the comparisons, since it had been applied in similar studies and took into account that the samples were dependent. The normality assumption was not met by the DEM pair differences, though, so the nonparametric counterpart, the Wilcoxon signed-rank test, was identified as an alternative test to perform.

At this point it is important to pause and briefly address the issue of spatial autocorrelation. Since geospatial data were considered in this analysis, it is highly likely that spatial autocorrelation was present in the DEMs. Waldo Tobler (1970) described spatial autocorrelation in what has become known as the First Law of Geography: “Everything is related to everything else, but near things are more related than distant things” (p. 236). This presents a problem when performing statistical analyses, because the independence of observations is typically an assumption found in classical statistics (Wong & Lee, 2005). Even though the paired *t*-test and Wilcoxon signed-rank test are meant for dependent samples, spatial autocorrelation may have affected the slope values. DEMs, even those of very high resolutions, are still generalizations of the actual terrain. It is therefore not surprising that errors are inherently present in DEMs when they are generated. These errors are autocorrelated and will propagate to any DEM derivatives, such as slope (Vaze et al., 2010). However, there is not a single, simple solution to address this challenge. Much research has been conducted using the Monte Carlo simulation technique to simulate error in order to research the spatial autocorrelation of

DEM errors (Wechsler & Kroll, 2006; Xuejun & Lu, 2008). Stochastic techniques have also been used (Stefanescu et al., 2012). If the differences between observations are spatially autocorrelated, it can lead to a greater chance of committing Type I errors (Warren et al., 2004). In statistics, Type I errors occur when the null hypothesis is rejected, when, in actuality, it should fail to be rejected. To address this challenge, one simple approach would be to only assess observations that are far enough apart to minimize the effects of spatial autocorrelation (in other words, look at a random subset of observations that are at least a specified distance from one another), but this approach potentially eliminates important information from the dataset. Even though spatial autocorrelation is not considered in this analysis, it is important to be aware of its potential effects so that corrections can be applied, if needed, at a future time.

The rejection of the normality assumption for the distributions of all the pair differences was not unexpected. The histograms show that the distributions do not follow a normal Gaussian bell-shaped distribution; rather, there is a tendency for the tails to be long and thin. This is due to the fact that the majority of the differences in slopes are not large, but there are a few pairs that do exhibit large positive and/or negative differences, causing the histograms to have long tails stretched in either a positive or negative direction. Kurtosis is the measure that describes this effect; a distribution with high kurtosis peaks at the mean and declines rapidly to heavy tails. The type of kurtosis readily seen in many of the histograms in Figures 22 through 24 is called leptokurtic, which is defined by a high peak in the middle and long tails on either side (Figure 25). While some of these large differences may be the result of outliers that had inaccurate slope values, it would not be appropriate to assume that all large differences could be removed simply to move closer to a normal distribution.

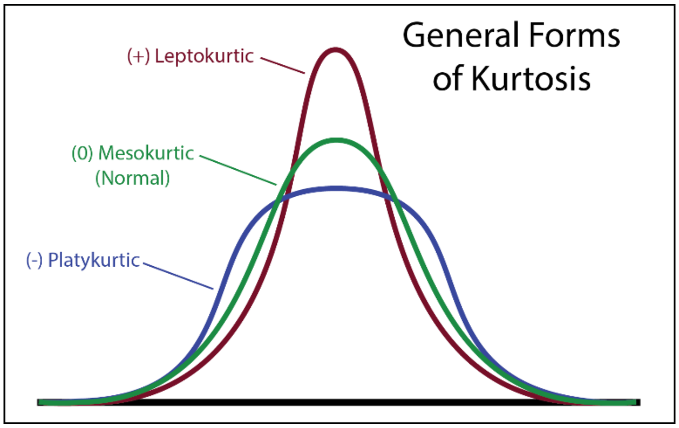

Figure 25 Kurtosis

It has been suggested that, even if the distributions are severely non-normal, it may still be alright to analyze the data using a parametric test, given that parametric tests are robust and not highly sensitive to non-normality (McDonald, 2014). If that were the case, and since the sample size was quite large, the paired *t*-test results could be considered acceptable on their own. Nevertheless, since both tests provided the same conclusions regarding every DEM pair, the objective of this research could clearly be answered. The lower resolution DEMs did not provide slope results comparable to those calculated using the high resolution 1 m DEM for this particular application and study area. Additionally, the lower resolution DEMs also did not provide results comparable to each other; in other words, the 5 m DEM could not be used in place of the 3 m DEM to deliver nearly the same slope results. This is primarily due to the scale of the application; higher resolutions are required to capture the level of detail needed.

CHAPTER SIX

6.1 Conclusions

The primary objective of this research was to determine if lower resolution elevation data could provide reasonably accurate slope values that could be incorporated into the GMU Geocrowdsourcing Testbed in order to improve dynamic routing solutions for visually and mobility impaired students. Slope results from three lower resolution DEMs (3 m, 5 m, and 10 m) were statistically compared, via paired *t*-tests and Wilcoxon signed-rank tests, to the slope results from a high resolution 1 m DEM, which had been deemed acceptable to use in the absence of ground truth data. The lower resolution DEMs were also compared to each other using the same statistical tests. The results of the paired *t*-tests and Wilcoxon signed-rank tests revealed that the differences between all DEM pairs, aside from the 3 m and resampled 3 m DEM pair, were statistically significant. Consequently, it was concluded that, for this type of application and at this scale, a high resolution (1 m or higher) DEM needs to be used for slope calculations, to provide the most accurate results for disabled pedestrian routing. The degree of variation in the topography of the GMU campus requires the use of the 1 m DEM to detect sidewalk slope changes, but if the study area had relatively little topographic variation, then a lower resolution DEM would likely be acceptable to capture the level of detail needed. In other words, based on the study area, as topography becomes more and more varied, DEM resolution would need to increase.

6.2 Future Work

While the RMSE results did show that the errors between the field surveyed spot elevations and the 1 m DEM elevations were minimal, it would be valuable to take a sample of field surveyed slopes across campus and compare those values to the slope values for the same sidewalk in the 1 m DEM. It may especially be worthwhile to field check the sidewalks that were in the strong slope category in Table 6 when the 1 m DEM was used, since there are only 20. Afterward, once corrections are made (if needed), slope values could be updated in the GMU Geocrowdsourcing Testbed's Pedestrian Network using values derived from the 1 m DEMs, since those DEMs are now available over the area, to provide the most accurate slope information. Further analysis should be conducted using the 1 m DEM to determine whether or not cross-slope could accurately be calculated and incorporated in the Pedestrian Network. However, the current Pedestrian Network only represents the centerline of sidewalks, and the lines on both sides of the sidewalk would be needed in order to calculate cross-slope.

Table 6 showed the number of line features in each maximum percent slope category. It would be interesting to be able to specify, when changing DEM resolutions, which line features changed from one category to another. Although it can already be observed that the number of features in the moderate and strong slope categories decreased as DEM resolution decreased, it would be beneficial to know if they switched to the next lowest slope category, or if they switched to an even lower category.

Several other modifications could be made to the Pedestrian Network to improve it. If time and resources allow, the network could be divided into shorter segments to more accurately capture sections where slope is too steep for disabled pedestrians. For example, if a 20 m sidewalk line contained a short segment at the end with a slope greater than 8.33%, the entire line would be classified as inaccessible (if maximum slope, versus average slope, were being considered). In reality, the pedestrian might need to only traverse 10 m of the sidewalk and then continue along another connected, accessible sidewalk. This possibility would not be identified by the routing algorithm, given that the entire sidewalk line would be eliminated from consideration. To minimize the total number of lines in the network in order to improve processing time, once slope has been calculated for short lines, adjacent lines with the same (or nearly the same) slope could be merged. Although, another motivation to keep line features shorter would be to not eliminate an entire sidewalk when routing is performed if only a portion of the sidewalk has an obstacle (dynamic information entered through crowdsourcing). That way, only the portion of the sidewalk with the obstacle would be classified as inaccessible. The optimal procedure for processing the Pedestrian Network would need to be finalized before it is included in the testbed application for routing to be performed.

To improve the user (pedestrian) experience with the routing results, it would be beneficial to allow the user to specify the maximum slope with which he or she is comfortable, since that is highly subjective. Additionally, since maximum slope preferences may be different depending on the direction of travel (uphill or downhill), the user would ideally have the option to specify constraints for maximum uphill (positive) slope and maximum downhill (negative) slope. These options would require that the routing algorithm be able to incorporate user-specified constraints. It would also require that the slope percentages in the attribute table of the Pedestrian Network be classified as positive or negative from the line start to end point. Laakso, T. Sarjakoski, Lehto, & L. Sarjakoski (2013) suggest that personal user accounts could be implemented so that profiles could be customized. For example, there could be profiles geared toward mobility impaired users, and profiles for visually impaired users. A feature layer of accessible entrances should be incorporated into the routing solution as well, to ensure that the recommend route leads to an accessible entrance. Even something as minimal as a single stoop, or small porch, in front of an entrance can prevent accessibility.

Another factor related to user preference is that of canopy cover. Recent research conducted by a student at GMU considered the possibility of selecting routes based on canopy cover (Heuwinkel, 2015). During warm months especially, disabled pedestrians may face thermoregulation challenges and prefer to travel in the shade. The canopy cover routing research did not take slope into account, so it would be beneficial to incorporate slope, verify the results, and then identify how to include that capability in the testbed. Ultimately, the success of an application, such as the GMU Geocrowdsourcing Testbed, is not simply measured by whether or not it accurately performs the functions for which it was designed. It is also measured by whether or not the application is intuitive and provides functionality that the user deems beneficial, in addition to providing trustworthy results.

REFERENCES

AnalystSoft Inc. (2015). StatPlus Professional for Windows (Build 5.8.9.5) statistical analysis program. Retrieved from https://www.analystsoft.com/en/products/statplus/

ArcGIS Desktop Advanced [GIS software]. (2014). Version 10.2.2. Redlands, CA: Environmental Systems Research Institute (ESRI), Inc.

Axelson, P. W., Wong, K. M., Lyons, C., Longmuir, P. E., Kirschbaum, J. B., Galvan, D. V., & Chesney, D. A. (1999). *Designing Sidewalks and Trails for Access. Part I of II: Review of Existing Guidelines and Practices*. United States Department of Transportation (DOT) Federal Highway Administration (FHWA). Retrieved from https://www.fhwa.dot.gov/environment/bicycle_pedestrian/publications/sidewalks

Barcelona Field Studies Centre. (2013). Measuring Slope Steepness. Retrieved from http://geographyfieldwork.com/SlopeSteepnessIndex.htm

Carswell, W.J., Jr. (2013). *The 3D Elevation Program—Summary for Virginia*. U.S. Geological Survey Fact Sheet 2013–3052, 2 p. Retrieved from http://pubs.usgs.gov/fs/2013/3052/

Ding, D., Parmanto, B., Karimi, H. A., Roongpiboonsopit, D., Pramana, G., Conahan, T., & Kasemsuppakorn, P. (2007). Design considerations for a personalized wheelchair navigation system. *Engineering in Medicine and Biology Society*, 4790-4793.

Elrod, D. (2015). Reporting the results of a t-test. Retrieved from http://www.csic.cornell.edu/Elrod/t-test/reporting-t-test.html

Environmental Systems Research Institute (ESRI). (n.d.). ArcGIS Help 10.2. Retrieved from http://resources.arcgis.com/en/help/main/10.2/

ESRI (2015). ArcGIS - World Imagery Map Service. Retrieved from https://www.arcgis.com/home/item.html?id=10df2279f9684e4a9f6a7f08febac2a9

ESRI (2015). ArcGIS - World Topographic Map Service. Retrieved from http://www.arcgis.com/home/item.html?id=30e5fe3149c34df1ba922e6f5bbf808f

ET GeoWizards for ArcGIS. (2014). Version 11.2. Retrieved from http://www.ianko.com/ET_GeoWizards/gw_main.htm

Federal Geographic Data Committee. (1998). Geospatial Positioning Accuracy Standards, Part 3: National Standard for Spatial Data Accuracy. *Subcommittee for Base Cartographic Data*.

Fairfax County. (n.d.). GIS & Mapping Services: Open Data. Retrieved from http://data.fairfaxcountygis.opendata.arcgis.com/

Fuchs, M., Torizin, J., & Kühn, F. (2014). The effect of DEM resolution on the computation of the factor of safety using an infinite slope model. *Geomorphology*, *224*, 16-26.

George Mason University (GMU). (2012). Campus Accessibility: Fairfax Campus - Physical Accessibility Map (PDF). Retrieved from http://accessibility.gmu.edu/campusAccess/upload/Fairfax-Campus-Accessibility-Map.pdf

Gillin, C. P., Bailey, S. W., McGuire, K. J., & Prisley, S. P. (2015). Evaluation of Lidar-derived DEMs through Terrain Analysis and Field Comparison. *Photogrammetric Engineering & Remote Sensing*, *81*(5), 387–396. Retrieved from http://doi.org/10.14358/PERS.81.5.387

Grohmann, C. H. (2015). Effects of spatial resolution on slope and aspect derivation for regional-scale analysis. *Computers & Geosciences*, *77*, 111-117.

Haneberg, W. C. (2008). Elevation errors in a LIDAR digital elevation model of West Seattle and their effects on slope-stability calculations. *Reviews in Engineering Geology*, *20*, 55-65.

Heuwinkel, J. R. (2015, November). *Thermoregulation of Mobility Impaired Individuals through Tree Canopy Preference Routing.* Geography and GeoInformation Science GIS Day Poster Presentation, Facilitator: Dr. Paul Delamater, George Mason University, Fairfax, VA.

James, T. D., Murray, T., Barrand, N. E., & Barr, S. L. (2006). Extracting photogrammetric ground control from lidar DEMs for change detection. *The Photogrammetric Record*, *21*(116), 312–328. Retrieved from http://doi.org/10.1111/j.1477-9730.2006.00397.x

Kasemsuppakorn, P., & Karimi, H. A. (2009). Personalised routing for wheelchair navigation. *Journal of Location Based Services, 3*(1), 24-54.

Laakso, M., Sarjakoski, T., Lehto, L., & Sarjakoski, L. T. (2013). An information model for pedestrian routing and navigation databases supporting universal accessibility. *Cartographica: The International Journal for Geographic Information and Geovisualization*, *48*(2), 89-99.

Li, J., & Wong, D. W. (2010). Effects of DEM sources on hydrologic applications. *Computers, Environment and Urban Systems*, *34*(3), 251-261.

Liu, X., Zhang, Z., Peterson, J., & Chandra, S. (2007). LiDAR-Derived High Quality Ground Control Information and DEM for Image Orthorectification. *GeoInformatica*, *11*(1), 37–53. Retrieved from http://doi.org/10.1007/s10707-006-0005-9

Lundberg, B., & Weber, J. (2014). Non-motorized transport and university populations: an analysis of connectivity and network perceptions. *Journal of Transport Geography*, *39*, 165-178.

McCrum-Gardner, E. (2008). Which is the correct statistical test to use? *British Journal of Oral and Maxillofacial Surgery*, *46*(1), 38–41. Retrieved from http://doi.org/10.1016/j.bjoms.2007.09.002

McDonald, J.H. (2014). Paired *t*-test. *Handbook of Biological Statistics*, 3rd ed. Sparky House Publishing, Baltimore, Maryland. Retrieved from http://www.biostathandbook.com/pairedttest.html

Mordkoff, J.T. (2011). *The Assumption(s) of Normality*. The University of Iowa, Iowa City, Iowa. Retrieved from http://www2.psychology.uiowa.edu/faculty/mordkoff/GradStats/part%201/I.07%20normal.pdf

National Oceanic and Atmospheric Administration (NOAA). (2006). *Ground Truth Survey for LiDAR Control: FY 2006 Rutland Ranch Topographic Mapping (SB19)*. Retrieved from ftp://ftp.csc.noaa.gov/pub/crs/beachmap/qa_docs/fl/swfwmd/Rutland_Ranch_Ground_Control_Report.pdf

Price, M. (2012). *Fire Mapping: Building and Maintaining Street Networks in ArcGIS*. Redlands, CA: Environmental Systems Research Institute (ESRI). Retrieved from http://www.esri.com/library/ebooks/fire-mapping-street-networks.pdf

Public Works Department, City of Clayton, Missouri. (2014). *Sidewalk and Curb Ramp ADA Self-Evaluation and Transition Plan*. Retrieved from http://www.claytonmo.gov/Government/Departments/Public_Works/ADA_Transition_Plan.htm

Qin, H., Rice, R. M., Fuhrmann, S., Rice, M. T., Curtin, K. M., & Ong, E. (2015). Geocrowdsourcing and accessibility for dynamic environments. *GeoJournal*, 1–18. Retrieved from http://doi.org/10.1007/s10708-015-9659-x

Rice, M. T., Curtin, K. M., Paez, F. I., Seitz, C. R., & Qin, H. (2013). *Crowdsourcing to Support Navigation for the Disabled: A Report on the Motivations, Design, Creation and Assessment of a Testbed Environment for Accessibility*. US Army Corps of Engineers, Engineer Research and Development Center, US Army Topographic Engineering Center Technical Report, Data Level Enterprise Tools Workgroup, George Mason University, Fairfax, VA. Retrieved from http://oai.dtic.mil/oai/oai?verb=getRecord&metadataPrefix=html&identifier=ADA588474

Rice, M. T., Curtin, K.M., Pfoser, D., Rice, R. M., Fuhrmann, S., Qin, H., Vese, R., Ong, E.W., Fayne, J.V., Paez, F. I., Seitz, C. R., Rice, M.A., & Yu, M. (2015). *Social Moderation and Dynamic Elements in Crowdsourced Geospatial Data*. US Army Corps of Engineers, Engineer Research and Development Center, Geospatial Research Laboratory Technical Report, George Mason University, Fairfax, VA.

Rice, M. T., Paez, F. I., Rice, R. M., Ong, E. W., Qin, H., Seitz, C. R., Fayne, J. V., Curtin, K. M., Fuhrmann, S., Pfoser, D., & Medina, R. M. (2014). *Quality Assessment and Accessibility Applications of Crowdsourced Geospatial Data: A Report on the Development and Extension of the George Mason University Geocrowdsourcing Testbed*. George Mason University, Fairfax, VA.

Routino - OpenStreetMap Wiki. (n.d.). Retrieved from http://wiki.openstreetmap.org/wiki/Routino

Samuels, M. L., Witmer, J. A., & Schaffner, A. (2012). *Statistics for the Life Sciences*. Fourth Edition, Prentice Hall, 2012.

Souleyrette, R., Hallmark, S., Pattnaik, S., O'Brien, M., & Veneziano, D. (2003). *Grade and Cross Slope Estimation from LIDAR-based Surface Models*. MTC-2001-02. Prepared by the Midwest Transportation Consortium at Iowa State University for the Research and Special Programs Administration, U.S. Department of Transportation: Washington, DC.

Stefanescu, E. R., Bursik, M., Cordoba, G., Dalbey, K., Jones, M. D., Patra, A. K., Pieri, D.C., Pitman, E.B., & Sheridan, M. F. (2012). Digital elevation model uncertainty and hazard analysis using a geophysical flow model. *Proceedings of the Royal Society of London A: Mathematical, Physical and Engineering Sciences*, *468*(2142), 1543–1563. http://doi.org/10.1098/rspa.2011.0711

Thompson, J. A., Bell, J. C., & Butler, C. A. (2001). Digital elevation model resolution: effects on terrain attribute calculation and quantitative soil-landscape modeling. *Geoderma, 100*(1–2), 67–89. Retrieved from http://doi.org/10.1016/S0016-7061(00)00081-1

Tobler, W. R. (1970). A Computer Movie Simulating Urban Growth in the Detroit Region. *Economic Geography*, *46*, 234–240. http://doi.org/10.2307/143141

United States Access Board. (n.d.). Chapter 4: Accessible Routes. *ADA Standards*. Retrieved from http://www.access-board.gov/guidelines-and-standards/buildings-and-sites/about-the-ada-standards/ada-standards/chapter-4-accessible-routes

United States Department of Transportation Federal Highway Administration. (2014). Designing Sidewalks and Trails for Access: Chapter 4 – Sidewalk Design Guidelines and Existing Practices. *Bicycle and Pedestrian Program*. Retrieved from https://www.fhwa.dot.gov/environment/bicycle_pedestrian/publications/sidewalks/chap4a.cfm

United States Geological Survey (USGS). (2015). The National Map: Elevation. Retrieved from http://nationalmap.gov/elevation.html

USGS. (2015). The National Map: 3D Elevation Program (3DEP). Retrieved from http://nationalmap.gov/3DEP/index.html

USGS. (2015). The National Map: 3DEP Product Metadata. Retrieved from http://nationalmap.gov/3DEP/3dep_prodmetadata.html

Vaze, J., Teng, J., & Spencer, G. (2010). Impact of DEM accuracy and resolution on topographic indices. *Environmental Modelling & Software*, *25*(10), 1086-1098.

Virginia Department of Conservation and Recreation. (n.d.). Overview of Physiography & Vegetation of VA. Retrieved from http://www.dcr.virginia.gov/natural-heritage/natural-communities/ncoverview

Warren, S. D., Hohmann, M. G., Auerswald, K., & Mitasova, H. (2004). An evaluation of methods to determine slope using digital elevation data. *Catena*, *58*(3), 215-233.

Waze. (n.d.). Segment length. Retrieved from https://wiki.waze.com/wiki/Segment_length

Wechsler, S. P., & Kroll, C. N. (2006). Quantifying DEM Uncertainty and its Effect on Topographic Parameters. *Photogrammetric Engineering & Remote Sensing*, *72*(9), 1081–1090. Retrieved from http://doi.org/10.14358/PERS.72.9.1081

Weih, R.C. & Mattson, T.L. (2004). Modeling Slope in a Geographic Information System. *Journal of the Arkansas Academy of Science*, *58*, 100-108. Retrieved from https://libinfo.uark.edu/aas/issues/2004v58/v58a16.pdf

White, R. A., Dietterick, B. C., Mastin, T., & Strohman, R. (2010). Forest Roads Mapped Using LiDAR in Steep Forested Terrain. *Remote Sensing*, *2*(4), 1120–1141. http://doi.org/10.3390/rs2041120

Wong, W. S. D., & Lee, J. (2005). *Statistical Analysis of Geographic Information with ArcView GIS and ArcGIS*. Wiley.

Xuejun, L. I. U., & Lu, B. (2008). Accuracy Assessment of DEM Slope Algorithms Related to Spatial Autocorrelation of DEM Errors. In Q. Zhou, B. Lees, & G. Tang (Eds.), *Advances in Digital Terrain Analysis* (pp. 307–322). Springer Berlin Heidelberg. Retrieved from http://link.springer.com/chapter/10.1007/978-3-540-77800-4_16

Zaiontz, C. (2015). Real Statistics Resource Pack software (Release 4.3). *Real Statistics Using Excel*. Retrieved from www.real-statistics.com

BIOGRAPHY

Robin E. Rodgers graduated from St. John Center for Independent Study in Atlanta, Georgia, in 2003. She received her Bachelor of Science in Geography from The University of Georgia in Athens, Georgia, in 2007. She was employed as a GIS Technician at the Center for Remote Sensing and Mapping Science in Athens, Georgia, before moving to the Washington, D.C. area in 2007 to work as a physical scientist for the U.S. Army Corps of Engineers.